To the Graduate Council:

I am submitting herewith a thesis written by Jackie T. Hill entitled "Clad Thickness Measurement Using Dual Frequency Eddy Current." I recommend that it be accepted in partial fulfillment of the requirements for the degree of Master of Science, with a major in Physics.

W. E. Deeds

Major Professor

We have read this thesis
and recommend its acceptance:

H. C. Schweinler

R. L. Becker

Accepted for the Council:

Dayton A. Smith

Vice Chancellor
Graduate Studies and Research

C

CLAD THICKNESS MEASUREMENT USING DUAL FREQUENCY EDDY CURRENT

A Thesis

Presented for the

Master of Science Degree

The University of Tennessee

Jackie T. Hill

December 1974

ACKNOWLEDGEMENTS

I wish to thank C. V. Dodd and W. E. Deeds for their guidance and time given throughout the scope of this experiment. I would also like to thank L. D. Chitwood for his assistance in setting up the instrumentation, and C. A. Reeves, Jr. for his help in programming the data processing and plot routines.

1176087

ABSTRACT

The purpose of this investigation was to determine the measurement accuracy of a dual-frequency eddy-current instrument for measuring the clad thickness of a conductor upon another conductor. The eddy-current instrumentation and measuring probe used were computer designed to minimize effects due to lift off and electrical conductivity (or resistivity) variations, and maximize the sensitivity to clad-thickness variations. The purpose of using two frequencies was to measure both the conductivity and thickness of the clads and to use the conductivity measurements to correct the thickness measurements for errors due to conductivity variations.

The experimental data were obtained from clads of two different conductivities and of various thicknesses. The base material had a conductivity value different from either of the clads. The resistivity ratios between the two different clad materials and the base material were approximately 1/2 and 1/3. The effect due to variation of lift off was minimized with a compensating circuit.

Responses from the measurements were in terms of voltage phase shifts. These phase shifts were later applied to a set of linear equations which were solved simultaneously to give an expression representing thickness. The constants in this expression were then set in a computer module, which plugs into the eddy-current instrumentation. The computer module used the constants and the measured phases to calculate the thickness of the clads.

It was determined that the dual-frequency technique measured clad thicknesses with better than a 99% accuracy. This accuracy is indicative of the thickness range incorporated in the phase responses applied to the set of linear equations.

TABLE OF CONTENTS

CHAPTER		PAGE
I.	INTRODUCTION	1
II.	THEORY	3
	Electromagnetic Induction	3
	Impedance Analysis	11
	Multiparameter Inspection	15
	Sources of Undesirable Effects Encountered in Eddy Currents	17
III.	CLADDING THICKNESS MEASUREMENT	21
	Introduction	21
	Apparatus	21
	Test Results	24
	Discussion of Errors	39
	Conclusions	42
BIBLIOGRAPHY		44
APPENDICES		46
APPENDIX A		47
APPENDIX B		50
VITA		62

LIST OF TABLES

TABLE		PAGE
I.	Eddy-Current Measurements of Clad C	26
II.	Eddy-Current Measurements of Clad D	27
III.	Summary of Data Taken for Resistivity Measurement	31
IV.	Summary of Data Taken from Cladding Measurements	33
V.	Cladding-Thickness Measurements with Reference at 40 mils and 9.63 Microhm-cm	36
VI.	Thickness and Resistivity Using Computer Unit	40
VII.	Summary of Thickness and Resistivity Measurements Using the Computer Unit	41

LIST OF FIGURES

FIGURE PAGE

1. Test Probe Above a Conductor 4
2. Test Probe in Air 5
3. Magnitude and Phase Angle of Coil Voltage 6
4. Simple Coil Circuit 7
5. Simplified Circuit Diagram for an Eddy-Current Reflection-Type Probe 9
6. Physical Arrangement of an Eddy-Current Probe Above a Conductor; Also, Electrical Connections in the Probe 10
7. Circuitry for the Impedance Analysis of a Probe Above a Conductor 12
8. Reactance Versus Resistance for Resistivity (or Conductivity) Variations 13
9. Reactance Versus Resistance for Thickness Variations 14
10. Phase Shift at Maximum Sensitivity for a 10% Cladding Thickness Change Versus Cladding Thickness/$\bar{r}$ for Various Conductivity Ratios 19
11. Two-Layer Thickness Loci 20
12. Dual-Frequency Configuration for the Modular, Phase-Sensitive Eddy-Current Instrument 22
13. Voltage Wave Form for Zero and Maximum Lift Off 25
14. Phase Shift Versus Resistivity for Clad C - Run 1 27
15. Phase Shift Versus Resistivity for Clad C - Run 2 28
16. Phase Shift Versus Resistivity for Clad C - Run 3 28
17. Phase Shift Versus Resistivity for Clad C - Run 4 29
18. Phase Shift Versus Resistivity for Clad D at 1 MHz 29
19. Phase Shift Versus Resistivity for Clad D at 2 MHz 30
20. Phase Shift Versus Resistivity for Clad D at 5 MHz 30

21. Thickness Versus Phase Shift at 20 KHz 37

22. Thickness Versus Phase Shift at 20 KHz with Reference at 40 mils 37

23. Thickness Versus Phase Shift at 200 KHz 38

24. Thickness Versus Phase Shift at 200 KHz with Reference at 40 mils 38

CHAPTER I

INTRODUCTION

Use of eddy-current for inspecting metal soundness, electrical properties, and thickness is widely used in many metal industries. This study investigated the thickness measurement of clads. Generally, there are two techniques used in the evaluation of clad thickness. The first technique evaluates the clad thickness as a function of a voltage magnitude change; the second technique determines clad thickness as a function of a voltage phase change or shift. Both techniques make use of a bridge circuit which is either operated in a balanced or unbalanced mode. That is, a change in thickness will either unbalance or balance the bridge circuit. Basically, what takes place in the operation of both techniques can be described simply as follows: an electromagnetic field is generated by an electromagnetic probe. When the probe is placed in the vicinity of a metallic test object, the electromagnetic field is modified by the electrical properties of the test object. The modified field is then sensed by the probe upon reflection from the test object. Presence of the reflected field causes a voltage change to be produced at a bridge circuit. This voltage changes the original balance or unbalance of the bridge which can be detected with an indicator. Of course, this simplified explanation omits the complicated details. More will be said about this operation later.

Both techniques, in addition to being sensitive to thickness variations, are sensitive to the electrical conductivity (or resistivity) and magnetic permeability of the metal, and to lift off (the distance between the measuring probe and the metal). However, the phase-sensing technique is not as sensitive to lift off as the magnitude technique. Variations in lift off encountered in the latter technique usually cause gross errors in the measurement of either of the other parameters just mentioned. The undesired response due to lift off may be electronically compensated for in the phase technique.

Phase-sensing eddy current has been further developed to include the simultaneous use of two or more electromagnetic fields at different frequencies. This multiple-frequency technique can be used to eliminate the response of one or more unwanted parameters while maximizing the response of a desired parameter. One example of this technique would be the measurement of a clad thickness using two different frequencies simultaneously. In such a case, a high and low frequency would be employed to measure resistivity and thickness, respectively.

This report describes an investigation involving the measurement of cladding thickness using the dual-frequency eddy current. Bronze was the cladding material used in this experiment. The clads were measured on a base material which will be referred to as Alloy-180. No practical application was considered in the use of these materials in this investigation. Two different bronze alloys with distinct resistivity values were measured separately on the Alloy-180 base. The resistivities of the two clads were determined experimentally with a single-frequency, phase-sensing, eddy-current system. A dual-frequency system was set up to measure the thickness variation of the cladding material upon the base. The frequencies used were determined with the aid of a computer program designed to help analyze eddy-current measurements of cladding thickness (Dodd, Cheng, Simpson, Deeds, Smith, 1973). The eddy-current-system parameters were determined by the same computer program.

The measured thickness values were analyzed and compared to the mechanical measurements.

CHAPTER II

THEORY

Electromagnetic Induction

The basic principle involved in the eddy-current inspection of a metal test object is electromagnetic induction. The test probe, which essentially is an electromagnet, generates a varying electromagnetic field. The direction and magnitude of the field depend, largely, on the geometry of the test probe. The test probes discussed here are of the reflection type. These probes usually consist of a metal core wound with a current-conductive wire, forming a circular coil. In this particular case, the magnitude of the generated field depends on the number of turns in the coil of wire and the magnitude of the current flowing in the wire. The varying electromagnetic field causes a varying current to be generated in an electrically conducting test object placed in the immediate vicinity of the probe. Just as in the probe, the current flowing in the test object generates a secondary field. If the test object is nonmagnetic, the secondary field will oppose the primary field generated by the probe. The extent of this opposition depends on the electrical conductivity and size of the test object, and on the operating frequency of the test probe. Figures 1 and 2 illustrate a test probe with and without a test object, respectively. Note that the primary field of the test probe above the test object has been drawn to indicate an effective reduction in magnitude due to the presence of the secondary field of the test object. In addition to a change in magnitude, the primary field also suffers a change in phase. The excitation current of the test probe above, in air, is in phase with the primary field of the test probe. A secondary field, which modifies the primary field, is generated as a result of the presence of the test object; thus, a change in phase between the modified primary field and the excitation current is the outcome, shown vectorially in Figure 3. Note also that the voltage of the test probe coil is changed. The

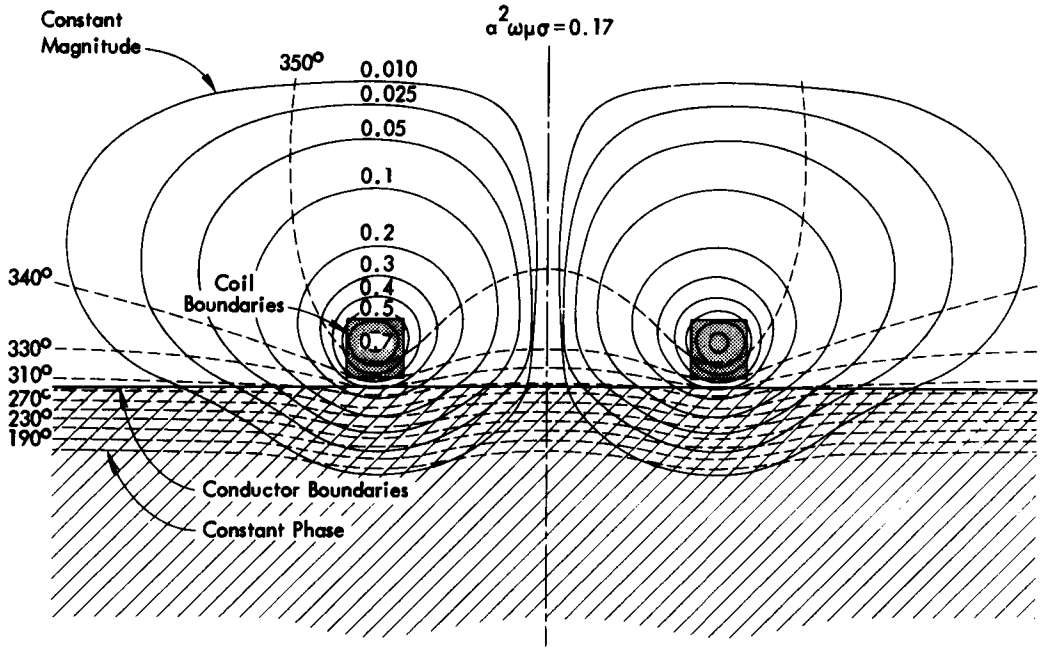
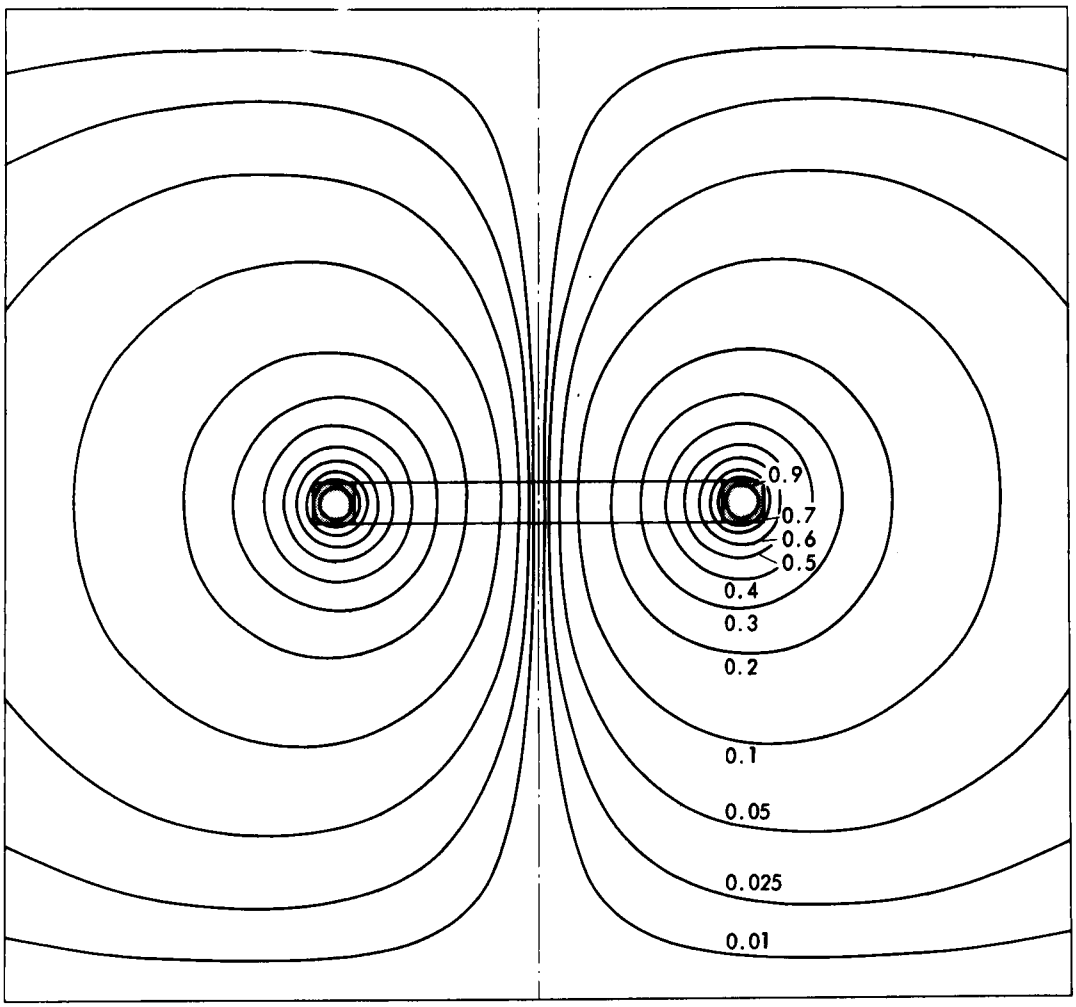


FIGURE 1

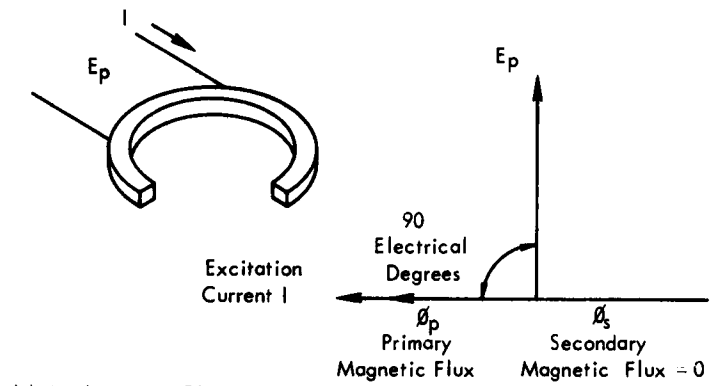
TEST PROBE ABOVE A CONDUCTOR



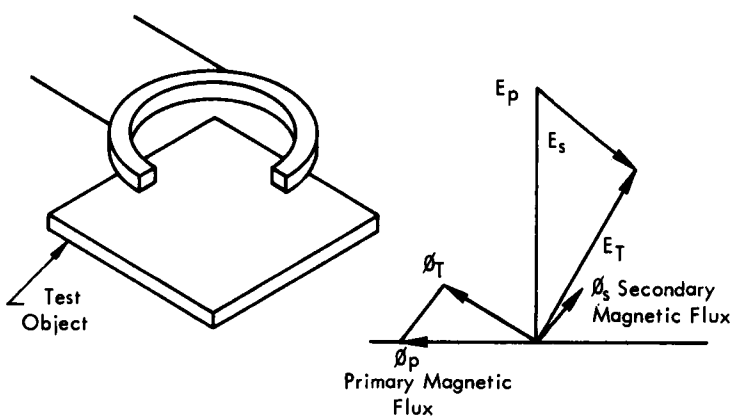
Magnitude Contours of an Electromagnetic Field

FIGURE 2

TEST PROBE IN AIR



(a) Without Test Object.



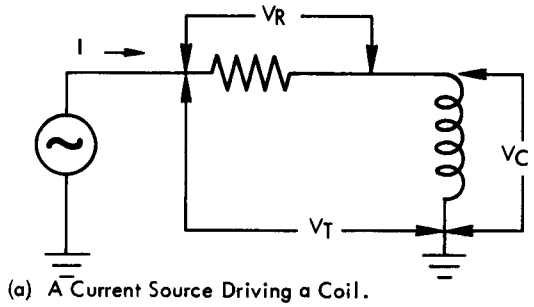
(b) With Test Object.

FIGURE 3

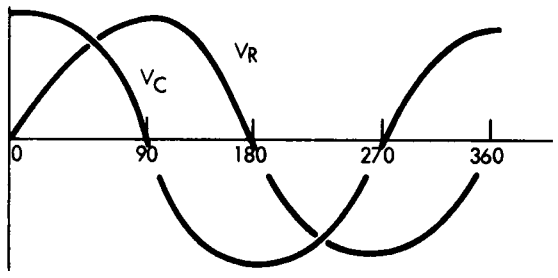
MAGNITUDE AND PHASE ANGLE OF COIL VOLTAGE

voltage, E_p, of the probe in air lags the excitation current, I, by 90 electrical degrees. The eddy currents induced in the test object generate a secondary magnetic field, ϕ_s, and its associated induced voltage, E_s, which lags the field by 90 electrical degrees. In Figure 3, the lagging direction is increasing in the clockwise direction. The vectorial sum of the two voltages is shown in the latter figure. The primary voltage, E_p, is usually subtracted from the total voltage, E_T, in practice. The lengths of the arrows represent the amplitudes of the voltages, while the directions represent the phases. It is these changes of voltage amplitude and phase that are measured in eddy-current inspection.

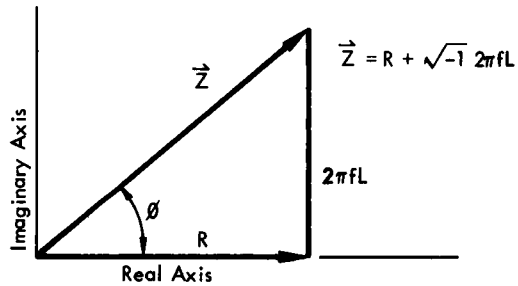
The primary coil voltage, E_p, is the product of the current, I, flowing through the coil and the total impedance, Z, across the coil circuit. A simple coil circuit may be represented, as noted in Figure 4(a). The impedance of the circuit can be divided into two components: the resistance (measure of the current opposition across the resistor in the circuit) and the reactance (measure of the circuit opposition across the inductance in the



(a) A Current Source Driving a Coil.



(b) Magnitude and Phase of the Voltages.



(c) Vector Impedance.

FIGURE 4

SIMPLE COIL CIRCUIT

circuit). The coil voltage, E_p, is actually the sum of the voltages across these two circuit components. As shown in Figure 4(b), the resistive component lags the reactive component by 90^o. Expressed vectorially, the voltage, E_p, is the vector sum of the resistive component, E_c. In terms of impedance, the vectorial representation may be diagrammed, as shown in Figure 4(c), where R is the resistance, X the reactance, and Z the impedance.

The value of the reactance is equal to the product of the angular frequency, $2\pi f$, and the inductance, L, of the circuit, thus:

$$X = 2\pi fL \ . \tag{1}$$

The impedance is then given by:

$$\begin{aligned} Z &= R + jX \\ &= R + j2\pi fL \ , \end{aligned} \tag{2}$$

where j represents the imaginary axis. The magnitude of the impedance is:

$$\begin{aligned} Z &= \sqrt{R^2 + X^2} \ , \text{ and the phase is:} \\ \theta &= \tan^{-1} \frac{X}{R} = \arctan \frac{X}{R} \ . \end{aligned} \tag{3}$$

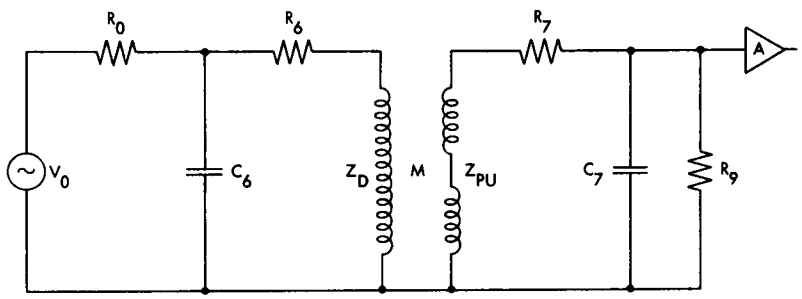
Dodd, Cheng, Simpson, Deeds, and Smith (1973) derived an expression for the voltage output of an eddy-current reflection-type probe. The expression is:

$$V_{out} = -j \frac{MV_0R_9G}{\omega C_6C_7} \div \left\{ \left(R_0 - \frac{j}{\omega C_6} \right) \omega^2 M^2 \left(R_9 - \frac{j}{\omega C_7} \right) \right.$$

$$+\left[\left(R_0-\frac{j}{\omega C_6}\right)\left(Z_0+R_6-\frac{j}{\omega C_6}\right)+\frac{1}{\omega^2 C_6^2}\right]$$

$$\times\left[\left(R_9-\frac{j}{\omega C_7}\right)\left(Z_{pu}+R_7-\frac{j}{\omega C_7}\right)+\frac{1}{\omega^2 C_7^2}\right]\Bigg\}. \qquad (4)$$

Figure 5 shows the simplified circuit diagram that was used in the derivation of this expression. Figure 6 shows a typical physical arrangement of a reflection-type probe above a conductor. Included in Figure 6 is a simplified circuit diagram of the same physical arrangement.



V_0	Driving Voltage
R_0	Series Resistance in the Driving Circuit
C_6	Shunt Capacitance of the Driving Circuit
R_6	DC Resistance of the Driver Coil
Z_D	Impedance of the Driver Coil
M	Mutual Impedance Between the Driver and Pickup Coils
Z_{PU}	Impedance of the Pickup Coils
R_7	DC Resistance of the Pickup Coils
C_7	Shunt Capacitance of the Pickup Circuit
R_9	Amplifier Input Impedance

FIGURE 5

SIMPLIFIED CIRCUIT DIAGRAM FOR AN EDDY-CURRENT REFLECTION-TYPE PROBE

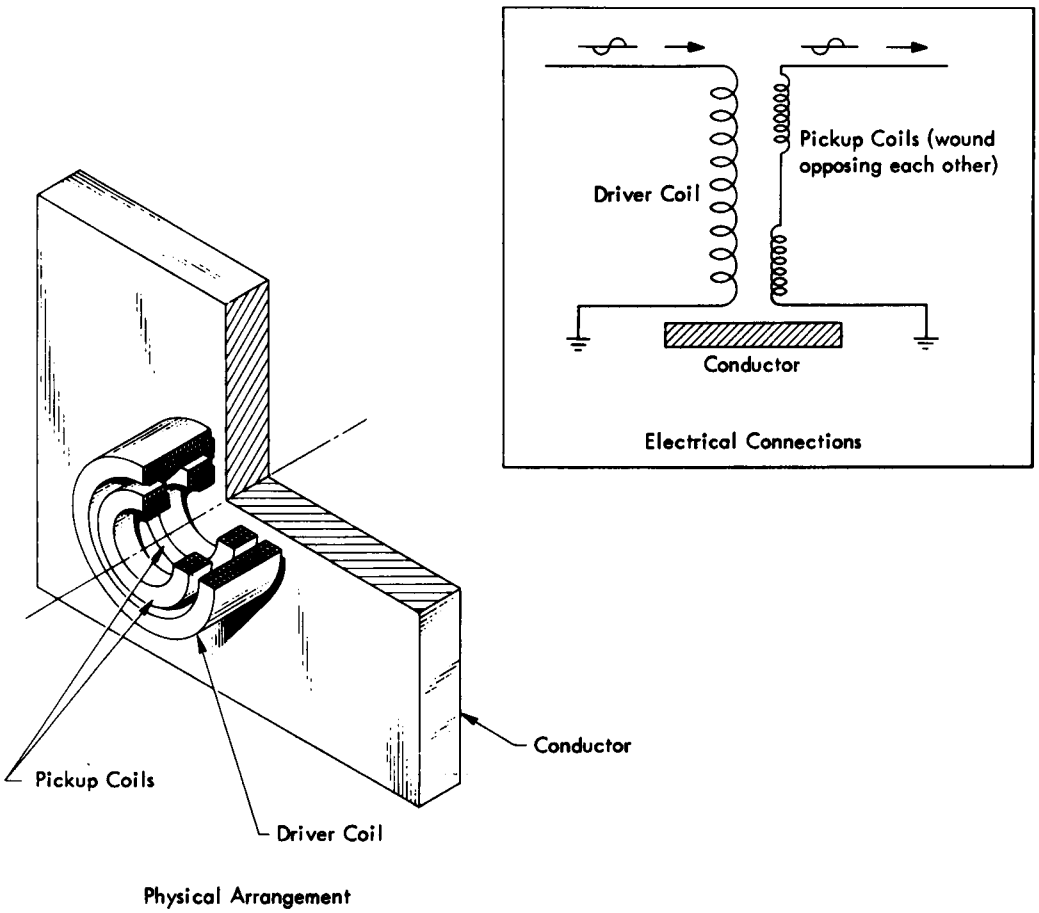


FIGURE 6

PHYSICAL ARRANGEMENT OF AN EDDY-CURRENT PROBE ABOVE A CONDUCTOR; ALSO, ELECTRICAL CONNECTIONS IN THE PROBE

Impedance Analysis

As mentioned earlier, the magnitude and phase of the primary voltage are usually subtracted from the measured coil signal. Let us, at this point, make an impedance analysis of a simple probe circuit placed above a secondary circuit of resistance R_2 and inductance L_2. The secondary circuit, for all practical purposes, represents a simple conducting loop. Figure 7(a) shows, schematically, the two circuits. The impedance of the primary coil can be found, as noted in Figure 4(c). If the secondary circuit parameters are added, the new phasor diagram would look like that shown in Figure 7(b). Here, the secondary resistance, R_2, is added to R_1, and the secondary inductance, L_2, is added to L_1. At the two limits of R_2; that is, at zero and infinity, the impedance is the same as that shown in Figure 4(c). However, as R_2 is varied from infinity to its zero value, the impedance vector, Z, will follow the path of a circular locus. Figure 8(a) shows such a locus. The same locus could also represent a variation in conductivity, since the resistivity is equal to the reciprocal of the conductivity. The electromagnetic coupling, M, between the two circuits causes a current to flow in the secondary circuit. The current flow sets up a secondary field which opposes and weakens the effect of the primary field. The inductive reactance sensed by the primary circuit is effectively decreased as a result of the decrease in the primary field strength. However, in the case of a solid conductor under the probe, the impedance locus follows a locus somewhat different from that shown in Figure 8(a). The locus looks more like that of Figure 8(b). This difference is due to the greater decrease of the reactance component of the impedance at decreasing resistivity (or increasing conductivity).

Let us turn our attention now to variations of thickness of a solid conductor under an eddy-current probe. Figure 9 shows a typical thickness locus. Note that the end with the high-conductivity value has more of a spiral-like shape than the conductivity locus shown in Figure 8. This variation in locus shape is due mainly to two factors—skin effect and shape of the probe coil. Both factors essentially reduce the current density in the conductor

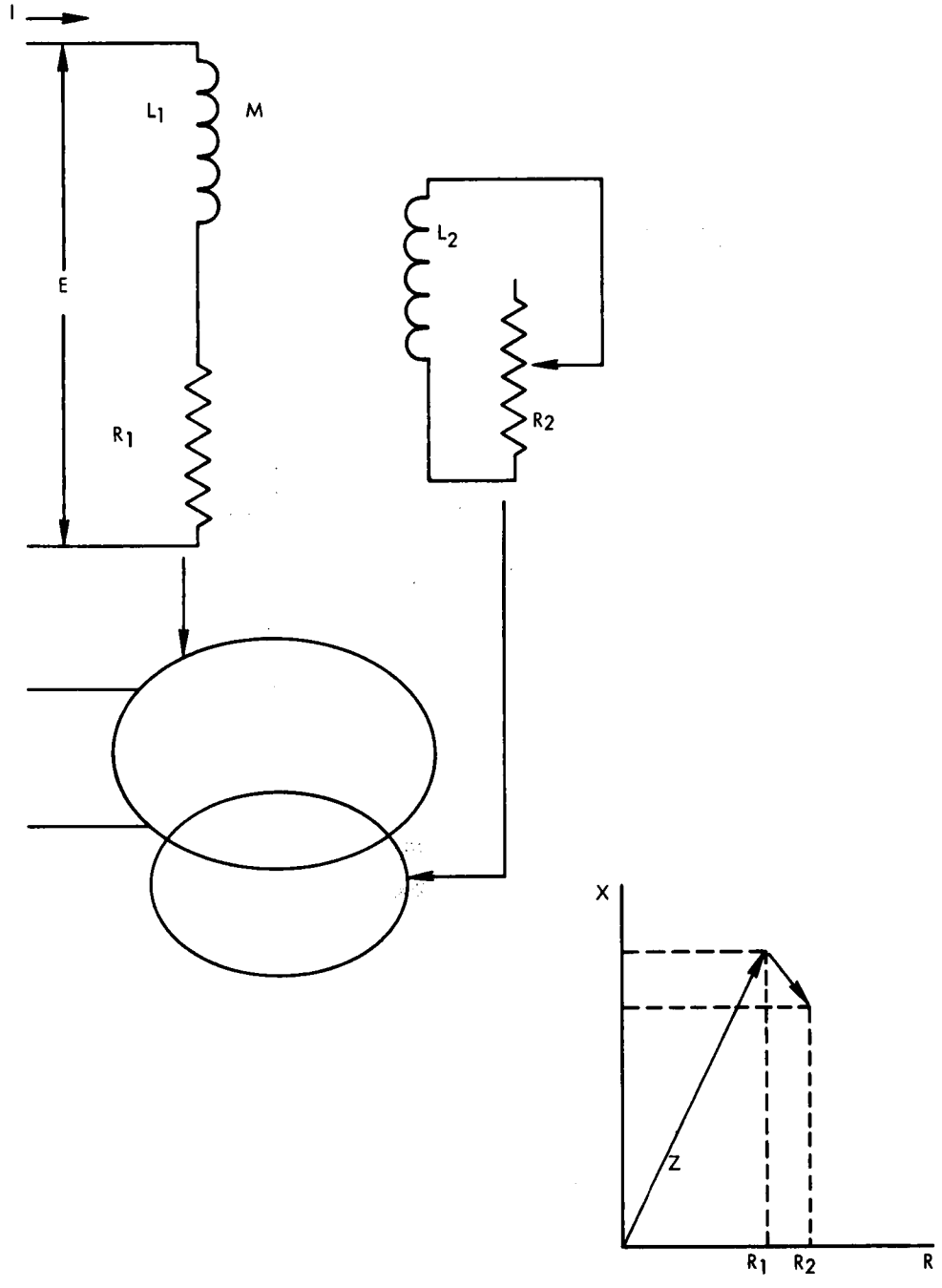
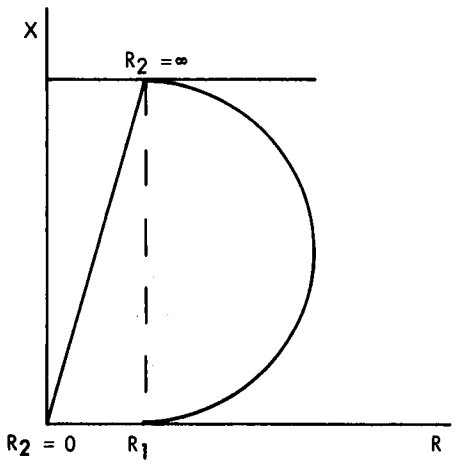
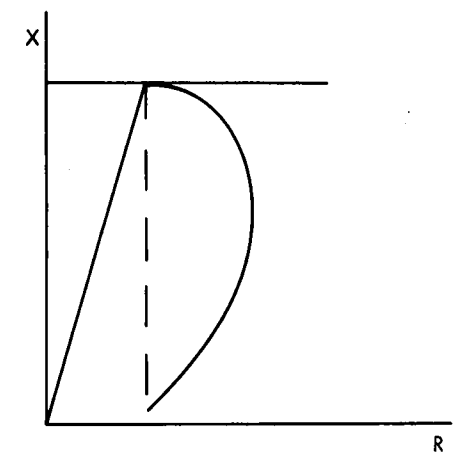


FIGURE 7

CIRCUITRY FOR THE IMPEDANCE ANALYSIS OF A PROBE ABOVE A CONDUCTOR



(a) Theoretical.



(b) Practical.

FIGURE 8

REACTANCE VERSUS RESISTANCE FOR RESISTIVITY (OR CONDUCTIVITY) VARIATIONS

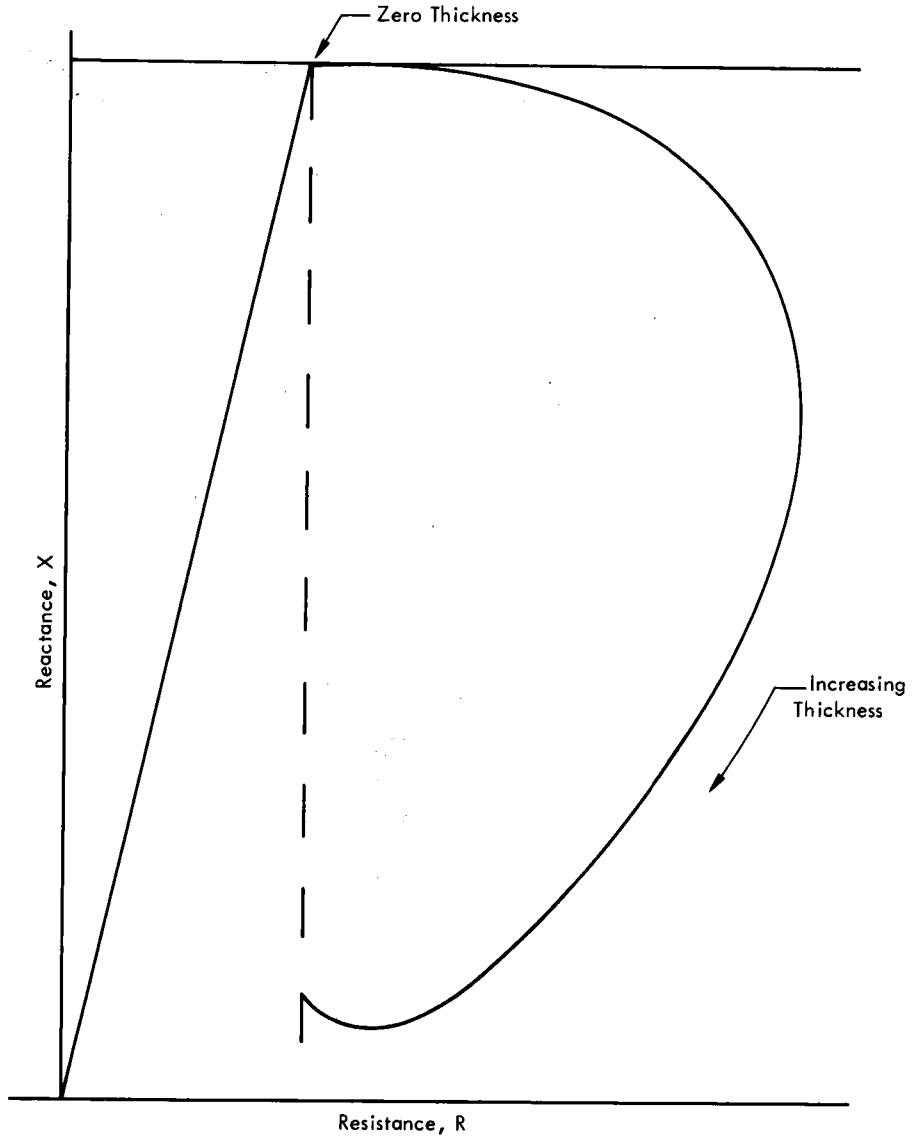


FIGURE 9

REACTANCE VERSUS RESISTANCE FOR THICKNESS VARIATIONS

as the depth below the surface increases. The current density decreases exponentially with increasing depth below the surface. The eddy currents generated in the conductor at some depth, X_a, produce a magnetic field at some greater depth, $X_a + \triangle X$. The field opposes the primary field, which weakens the current flow. The current flow gets progressively weaker as the depth of the magnetic field penetration increases. The current density at any depth, X, can be expressed by:

$$J_X = J_O \, \text{Exp}\left(-X\sqrt{\pi f \mu \sigma}\right)$$

where J_O represents the current density at the surface, f the probe operating frequency, μ the magnetic permeability of the conductor, and σ the conductivity of the conductor. The decrease in current density due to depth is associated with the skin effect; reduction due to the coil shape is caused by a cancellation effect on the current flowing on both sides of the coil. The more symmetric the coils, the more cancellation takes place. The majority of the spiraling is due to the skin effect.

Multiparameter Inspection

Variation in phase with a variation in the resistivity and thickness over a 10% range is fairly linear. Response of both these variables may be represented by linear equations. As mentioned previously, the difference in the phase of the input and output voltages is measured to indicate the value of a parameter using the phase-sensing eddy-current technique. The linear equations, thus, express a relation between the two said variables and their phase-shift response. The equations may be written as:

$$P_h = t\,T_h + \rho\,S_h, \text{ and} \qquad (5)$$

$$P_l = t\,T_l + \rho\,S_l\,, \tag{6}$$

where P_h and P_l represent the phase at high and low frequencies, respectively, T_h and T_l represent the linear response of the phase shift with thickness at high and low frequencies, S_h and S_l represent the linear response of the phase shift with resistivity (or conductivity) at high and low frequencies, and t and ρ represent the thickness and resistivity, respectively. The two equations may be solved simultaneously for either t or ρ as follows:

$$t = \frac{\begin{vmatrix} P_h & S_h \\ P_l & S_l \end{vmatrix}}{\begin{vmatrix} T_h & S_h \\ T_l & S_l \end{vmatrix}} = \frac{P_h S_l - P_l S_h}{T_h S_l - T_l S_h}\,, \text{ or} \tag{7}$$

$$\rho = \frac{\begin{vmatrix} T_h & P_h \\ T_l & P_l \end{vmatrix}}{\begin{vmatrix} T_h & S_h \\ T_l & S_l \end{vmatrix}} = \frac{T_h P_l - T_l P_h}{T_h S_l - T_l S_h}\,. \tag{8}$$

Thus, the measurement of one variable may be made completely independent of the other. The constants T_h, T_l, S_h, and S_l must be determined, however, by computer calculation or by experimental measurements of known conductors. Once these constants are found, Equations 7 and 8 may be written as:

$$t = a_1 P_h - a_2\,P_l, \text{ or} \tag{9}$$

$$\rho = a_3\,P_l - a_4\,P_h\,, \tag{10}$$

where:

$$a_1 = \frac{S_l}{T_h S_l - T_l S_h} ,$$

$$a_2 = \frac{S_h}{T_h S_l - T_l S_h} ,$$

$$a_3 = \frac{T_h}{T_h S_l - T_l S_h} , \text{ and} \qquad (11)$$

$$a_4 = \frac{T_l}{T_h S_l - T_l S_h} .$$

Sources of Undesirable Effects Encountered in Eddy Currents

As mentioned previously, the phase-sensing eddy-current technique produced less error due to lift-off variation than the magnitude technique. Lift off is usually the main undesirable variable encountered in thickness measurements. Such factors as metal surface finish, tilting of the measuring probe, and surface flatness cause changes in the probe-to-conductor spacing, or lift off. Such factors are also common in industrial thickness measurement setups.

One other factor that causes large errors in thickness measurements using the magnitude technique is variation in the coil d.c. (direct current) resistance. At low frequencies, the d.c. resistance of the coil can be as high as its impedance value. Again, the phase-sensing technique minimizes the thickness-measurement error due to such variations.

Now, a discussion of the error in thickness measurement due to variations in metal conductivity will be discussed. It should be pointed out here that a cladding thickness measurement is the measurement of the thickness of one conductor upon another. Measurements of a conductive coating on a conductor, and a conductor placed atop another

conductor are examples of cladding-thickness measurements. The greater the ratio between the conductivities of the conductors, the greater the measuring sensitivity to the cladding thickness. C. V. Dodd's report (1972) shows, graphically, how the thickness-measuring sensitivity varies with the conductivity ratio of the cladding material and the base material. Figure 10 simply combines several of Dodd's graphs to show this variation. Ratios of 10, 2, 1.25, 0.5, and 0.1 are shown here. As shown on the graph and pointed out in the report, there is adequate sensitivity when the conductivity ratios are as close to 1 as 1.25. The curves on the graphs represent the phase shift at maximum sensitivity for a 10% cladding-thickness change versus cladding thickness divided by the probe radius, r, for various conductivity ratios. These curves also depict some other very important factors in eddy-current-cladding thickness measurements. These are discussed in Dodd's report. Note that, on the graph, there are two inverse pairs; that is, 10 and 0.1 and 2 and 0.5. This, of course, simply means in one case a more-conductive metal was placed upon a less-conductive base (ratios 10 and 2). In the other case, a less-conductive metal was placed upon a more-conductive base (ratios 0.1 and 0.5). An impedance analysis can be made to depict these two cases. Let us assume that Metal A is more conductive than Metal B (Figure 11). When Metal A is placed upon Metal B and increases in thickness, the impedance point moves along the Curve AB from B to A; when Metal B is placed upon Metal A and increases in thickness, the impedance point moves along the curve BA from A to B. In either case, the base metal is sensed by the measuring probe until the cladding metal is too thick to penetrate.

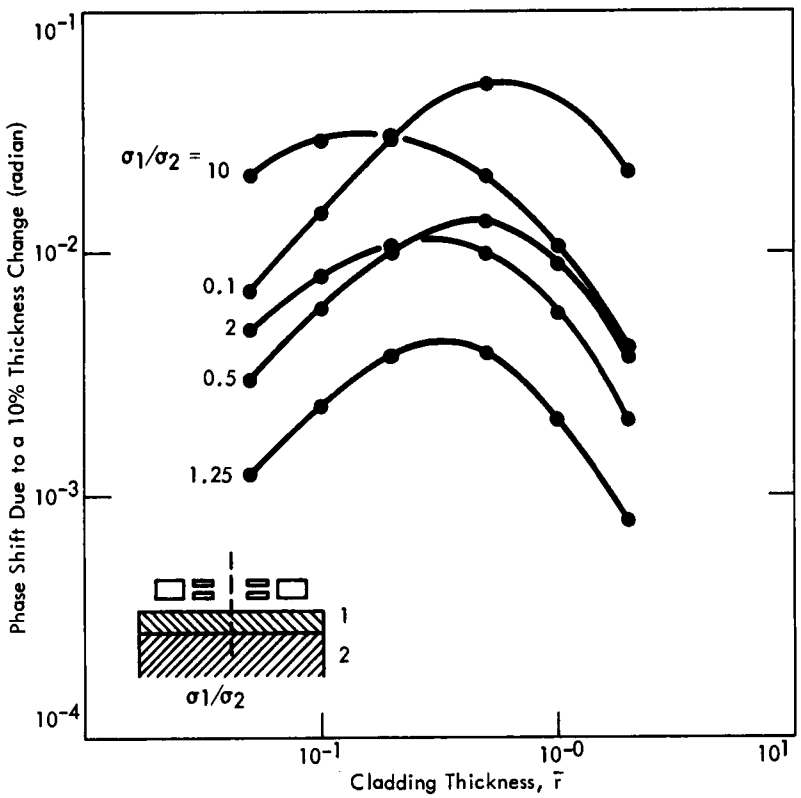


FIGURE 10

PHASE SHIFT AT MAXIMUM SENSITIVITY FOR A 10% CLADDING THICKNESS CHANGE VERSUS CLADDING THICKNESS/$\bar{r}$ FOR VARIOUS CONDUCTIVITY RATIOS

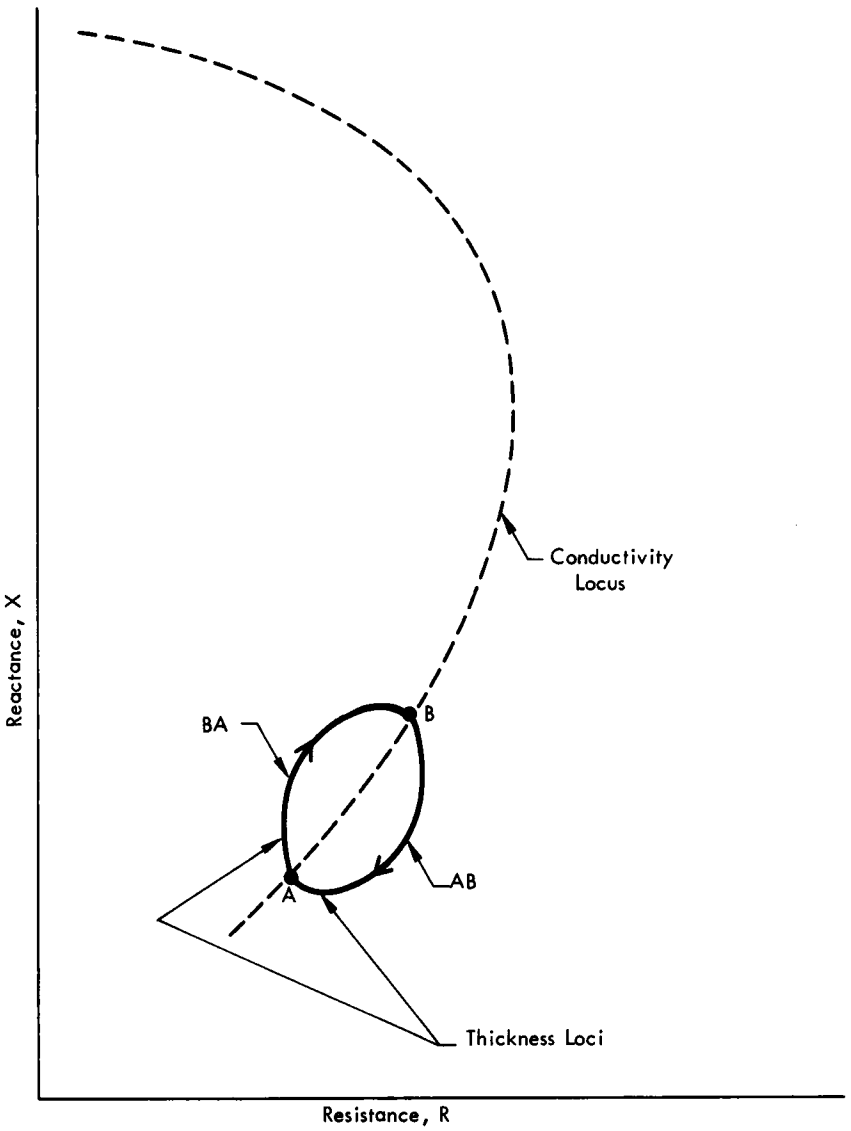


FIGURE 11

TWO-LAYER THICKNESS LOCI

CHAPTER III

CLADDING THICKNESS MEASUREMENT

Introduction

A computer-designed probe and eddy-current system were used to measure the cladding thickness of two different bronze samples on a base material. The base material, which will be referred to as Alloy 180, had an electrical resistivity value of 28.22 microhm-cm. Electrical resistivities of the two bronze claddings were determined experimentally. The claddings, which will be referred to as Clad C and Clad D, were found to have resistivity values of 15.56 and 9.63 microhm-cm, respectively. Following the resistivity determinations, each cladding thickness was measured using a dual-frequency eddy-current system.

Apparatus

A modular, dual-frequency, phase-sensitive eddy-current system was used to make the cladding-thickness measurements in this investigation. Figure 12 presents a block diagram of the instrument. The oscillator and power-amplifier module provides signals for excitation of the driver coil in the probe. This stable sinusoidal voltage signal passes through an attenuator before reaching the eddy-current probe. The probe and cladding conductor are physically arranged, as shown in Figure 6 (Page 10). The signals fed to the driver coil induce currents within the cladding conductor at two different frequencies. The cladding conductor, in turn, generates a secondary electromagnetic field which modifies the primary field and signal at the driver coil. This action modulates the pickup coil output signal. The modulated signal carries with it information about the condition of the cladding conductor.

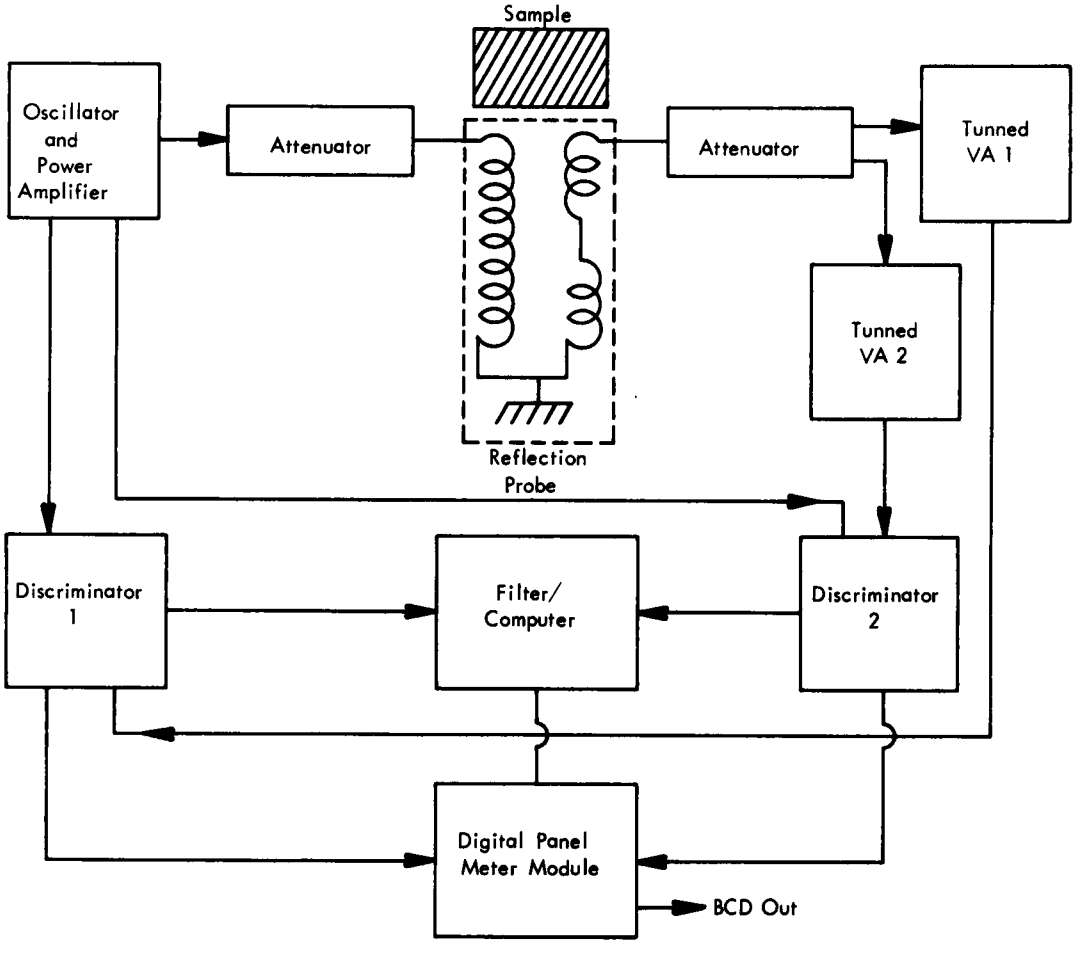


FIGURE 12

DUAL-FREQUENCY CONFIGURATION FOR THE MODULAR, PHASE-SENSITIVE EDDY-CURRENT INSTRUMENT

The pickup coil output signal passes through another attenuator into a video amplifier where it is amplified to a suitable magnitude.

The oscillator and power amplifier module, in addition to providing a signal to the driver coil, simultaneously feeds a signal to the discriminator. The discriminator (a compensating circuit) makes it possible to adjust the signal from the video amplifier. Since the same signal that goes to the driver coil is fed to the discriminator, the latter circuit can be adjusted to null out the signal received from the video amplifier. The phase shift between the reference input voltage signal and the detected output voltage signal is measured in the discriminator. Since the initial input signal carries two frequencies, two discriminators and two video amplifiers were used.

The signals from the two discriminators are then fed to a filter-computer module and a digital panel. At this stage, the signals are separated by wave filters having passbands centered at the two excitation frequencies. A fixed set of four predetermined constants are set in on the front panel of the computer module. The computer uses these constants, along with the measured phase shift, to calculate the cladding thickness and conductivity. Equations 7 and 8 represent the transformation from phase-shift response to the calculated parameters—thickness and conductivity, respectively. The calculated parameters are then fed to the digital panel meter where they are displayed for recording.

Following is a list of the specific modules used in this investigation:

1. Dual-Frequency Oscillator and Power Amplifier (DPA-2) - This unit provides a stable, low-distortion signal with an amplitude of 10 volts peak to peak and a frequency range from 1 KHz to 5 MHz.
2. Video Amplifiers (VA-206-T and VA-212-T) - These units amplify the low-level signals from the test probe to voltage levels that would drive the discriminator.

3. Discriminators (Disc 204 and Disc 102) - These units generate a d.c. voltage that is proportional to the phase shifts between the signals from the power amplifiers and the signals from the video amplifiers. The discriminator level was variable between zero and ± 10 volts.

In addition to the variable voltage levels on the two discriminators, there is also a lift-off compensator. This portion of the discriminator allows the adjustment of the voltage trigger level to be at some point slightly above the zero level, which minimizes the effect of lift off. This fact may be better understood if stated as follows: As the probe-to-cladding distance is varied (say, due to surface finish), a large change in the voltage amplitude is produced and a small change in the voltage phase. Normally, the phase shift between the input and output voltages is measured at the point where the voltage passthrough is zero. However, when lift off is encountered, the original input phase shifts slightly. The discriminator can now be set to trigger at a point where the maximum and zero lift offs have the same phase shift. This relationship is illustrated in Figure 13. In the figure, V_1 represents the point at which the voltage discriminator triggers.

Test Results

Resistivities of the bronze samples were determined with a single-frequency, phase-sensing eddy-current system. The reflection-type probe had a driver coil with a mean radius of 40 mils and pickup coils with mean radii of 21 mils. The system was calibrated to read in degrees directly with the aid of an RLC calibrator circuit. The circuit was plugged into the connector where the test probe is used. The circuit was equipped with a switch with dial positions ranging from 0 to ± 80.00 degrees in 10-degree increments. Also included were positions for ± 0.5, ± 79.5, and ± 80.5 degrees. The system was then calibrated for resistivity

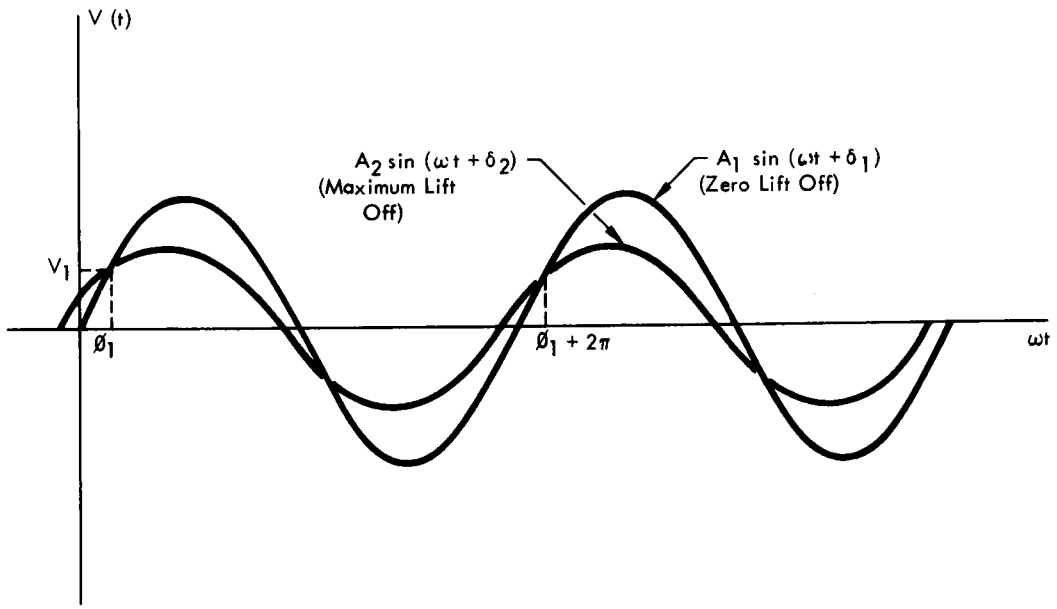


FIGURE 13

VOLTAGE WAVE FORM FOR ZERO AND MAXIMUM LIFT OFF

measurement using seven known standards whose resistivities ranged from 1.726 (copper) to 50.106 microhm-cm (constantan). The seven standards and their resistivities are:

Standard	Resistivity (microhm-cm)
Copper	1.726
1100 Aluminum Alloy	2.934
6061 Aluminum Alloy	3.474
2024 Aluminum Alloy	3.687
60 Alloy	9.727
180 Alloy	28.220
Constantan	50.106

A lift off of 3 mils was set in the lift-off compensation circuit. This setting was accomplished by placing a 3-mil shim on the constantan standard and adjusting the lift-off circuit to balance a minimum (without shim) and maximum (with shim) lift off.

Tables I and II contain the data taken from this part of the investigation. Each set of data was made with a different calibration. Figures 14 through 20 provide plots of each set of data fitted to a second-order, least-squares fit. Each of the curves was generated by plotting the log of the standard resistivities against the measured phase shifts. Log of the resistivity versus phase shift is approximately linear over a large resistivity variation. Frequencies of 1, 2, and 5 MHz were used to obtain the data given in Tables I and II. Each set of runs taken on the two bronze samples was statistically analyzed. Results of this analysis are given in Table III. The averages of the two bronze clads—Clad C and Clad D—were found to be 15.560 and 9.630 microhm-cm, respectively.

Table I

EDDY-CURRENT MEASUREMENTS OF CLAD C

Measurement Number	Phase Shift (degrees)			
	2 MHz			1 MHz
	Run 1	Run 2	Run 3	Run 4
1	-16.66	-16.76	-17.01	-23.85
2	-16.60	-16.60	-16.82	-23.65
3	-16.62	-16.75	-17.01	-23.88
4	-16.48	-16.59	-16.95	-23.77
5	-16.67	-16.77	-16.99	-23.86
6	-16.48	-16.60	-16.84	-23.62
7	-16.69	-16.72	-17.02	-23.81
8	-16.48	-16.55	-16.84	-23.62
9	-16.62	-16.72	-17.01	-23.82
10	-16.51	-16.66	-16.86	-23.61

Table II

EDDY-CURRENT MEASUREMENTS OF CLAD D

Measurement Number	Phase Shift (degrees)		
	1 MHz	2 MHz	5 MHz
1	-18.43	-13.80	-10.48
2	-18.41	-13.70	-10.44
3	-18.34	-13.78	-10.51
4	-18.50	-13.80	-10.55
5	-18.42	-13.77	-10.45
6	-18.48	-13.74	-10.42

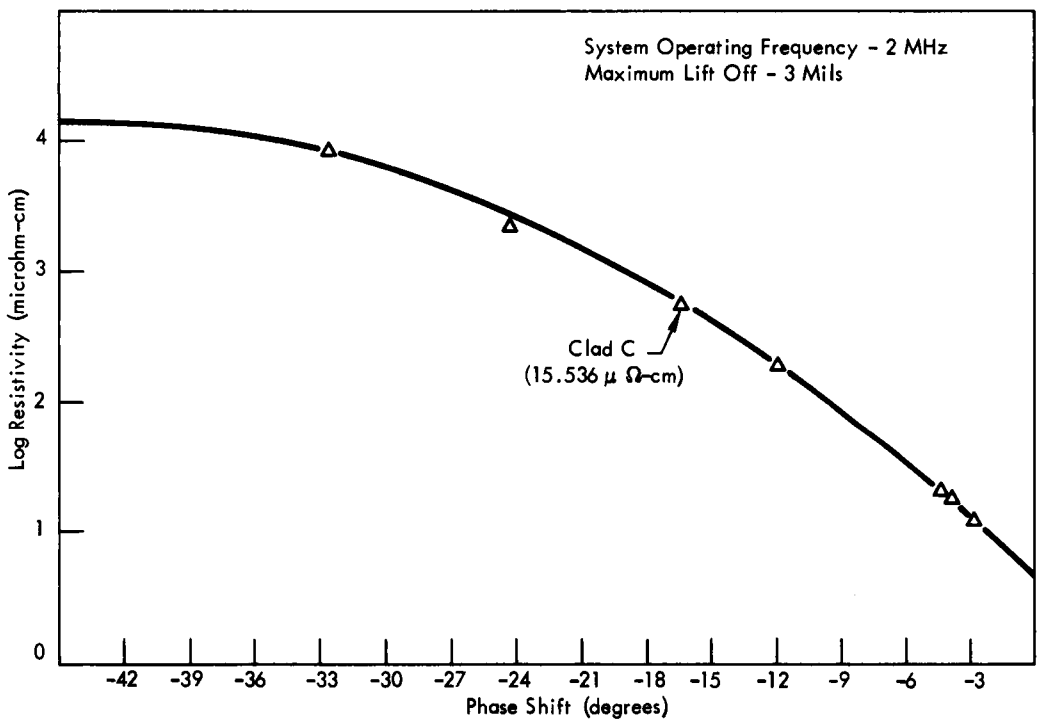


FIGURE 14

PHASE SHIFT VERSUS RESISTIVITY FOR CLAD C · RUN 1

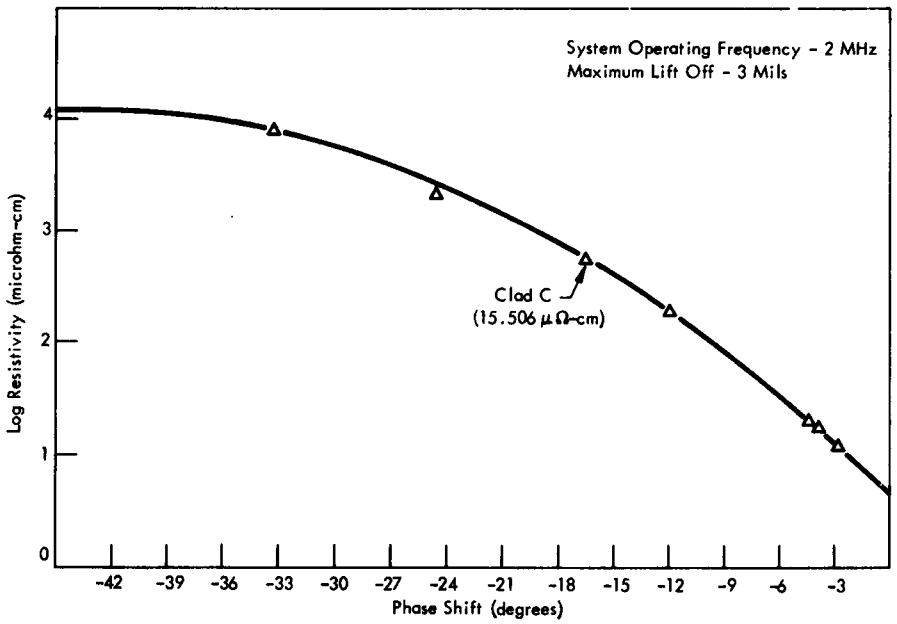


FIGURE 15

PHASE SHIFT VERSUS RESISTIVITY FOR CLAD C - RUN 2

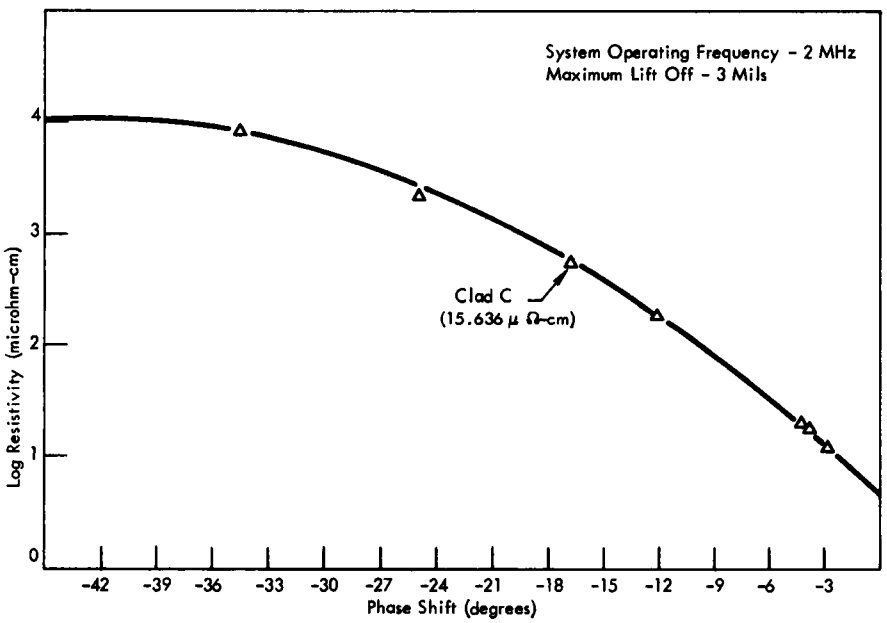


FIGURE 16

PHASE SHIFT VERSUS RESISTIVITY FOR CLAD C - RUN 3

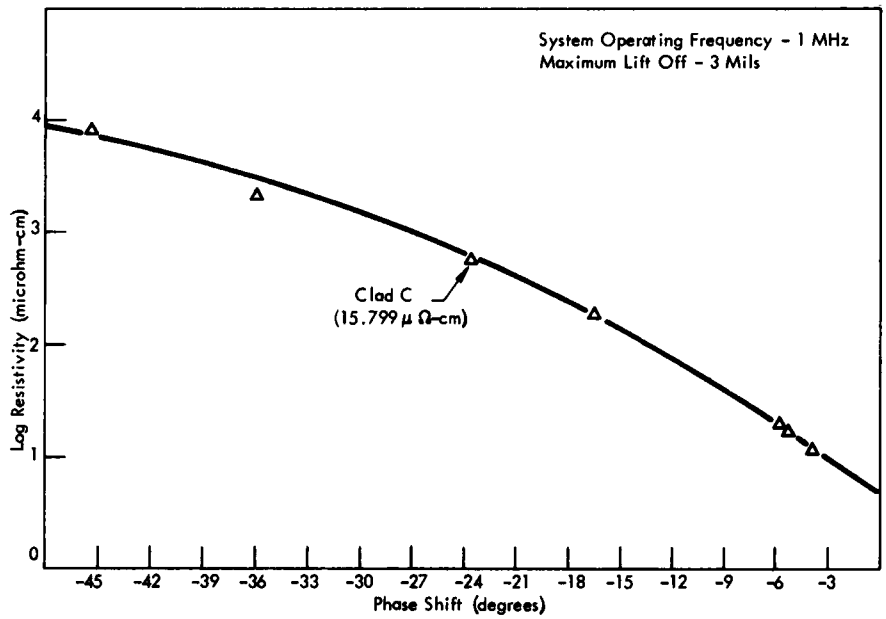


FIGURE 17

PHASE SHIFT VERSUS RESISTIVITY FOR CLAD C - RUN 4

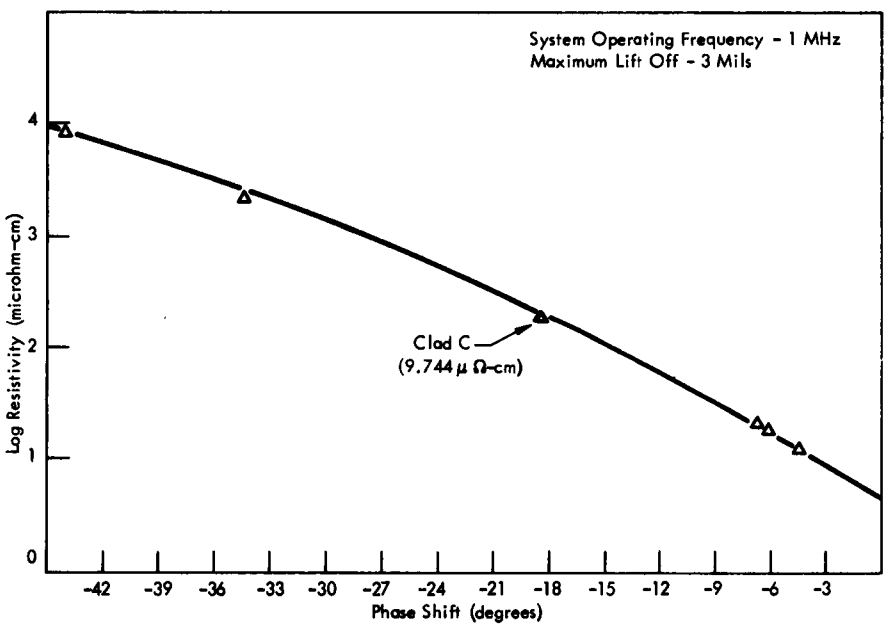


FIGURE 18

PHASE SHIFT VERSUS RESISTIVITY FOR CLAD D AT 1 MHz

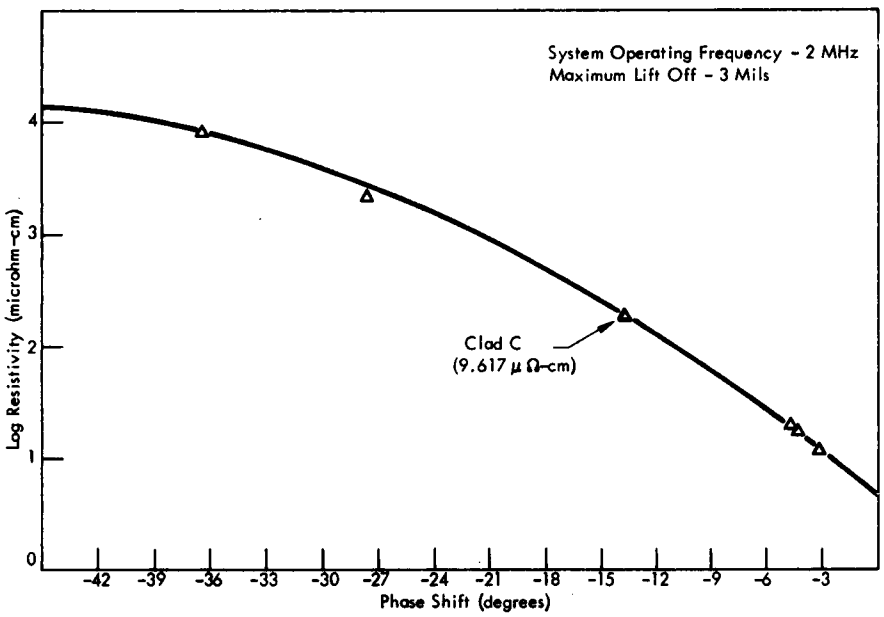


FIGURE 19

PHASE SHIFT VERSUS RESISTIVITY FOR CLAD D AT 2 MHz

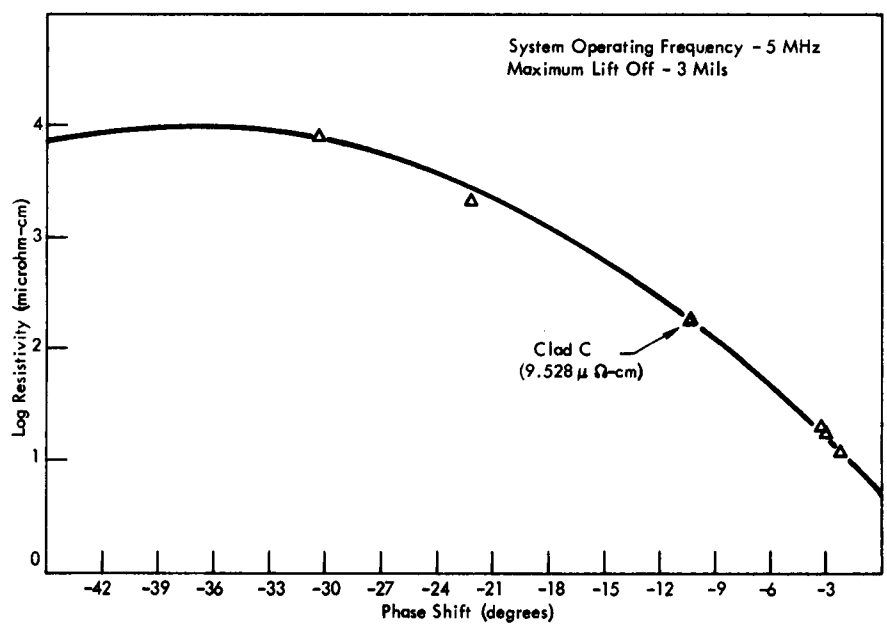


FIGURE 20

PHASE SHIFT VERSUS RESISTIVITY FOR CLAD D AT 5 MHz

Table III

SUMMARY OF DATA TAKEN FOR RESISTIVITY MEASUREMENT

Sample Run	Frequency (Hz)	Average Phase Shift (degrees)	Standard Deviation	95 Percent Confidence Limits	Calculated Resistivity (microhm-cm)	Standard Deviation
Clad C Run 1	2M	- 16.581	0.085	0.053	15.536	0.13
Clad C Run 2	2M	- 16.672	0.082	0.051	15.383	0.12
Clad C Run 3	2M	- 16.935	0.084	0.052	15.636	0.13
Clad C Run 4	1M	- 23.749	0.111	0.069	15.799	0.12
Clad D Run 1	1M	- 18.430	0.056	0.045	9.744	0.04
Clad D Run 2	2M	- 13.765	0.039	0.031	9.617	0.04
Clad D Run 3	5M	- 10.475	0.048	0.039	9.528	0.06

After determining the resistivities of the two bronze claddings, the constant values in Equation 7 in the theory portion of this thesis were determined. As mentioned previously, all of the system parameters, including the operating frequency, were determined by computer. For maximum thickness sensitivity, the two frequencies chosen were 20 and 200 KHz. These two frequencies were set on the dual-frequency eddy-current oscillator and power amplifier.

To determine the constants in Equation 11, several sets of measurements were made to find the phase-shift values corresponding to the change of thickness and conductivity on the two claddings. The eddy-current system was divided into two channels: the low frequency (20 KHz) was set on Channel 1, the high frequency (200 KHz) was set on Channel 2. Each channel consisted of a video amplifier and discriminator. Each channel fed through the latter two circuits into the filter computer and digital panel meter. The signal to the digital panel meter was selected by a six-position rotary switch. However, for the purpose of this investigation, only four of the six positions were used. The positions labeled Phase 1 and Phase 2 were used to obtain the signal from the discriminators of Channels 1 and 2, respectively. (The other two positions used in this investigation will be discussed later.) Channel 1 was used to monitor the phase shifts corresponding to thickness changes; Channel 2 to monitor conductivity.

After the system was calibrated (as described previously) and lift off set for a maximum variation of 3 mils, each cladding was placed (one at a time) on the base material. Three different thicknesses of Clad C (15.56 $\mu\Omega$-cm) were measured for phase shifts on the two channels. Two thicknesses of Clad D (9.63 $\mu\Omega$-cm) were measured. Table IV contains the data taken from these measurements. Note in Table IV that the variation in phase shift using 200 KHz is much less than that using 20 KHz. This difference, of course, is due primarily to the fact that the electromagnetic field is concentrated more at the surface of

Table IV

SUMMARY OF DATA TAKEN FROM CLADDING MEASUREMENTS

Measurement Number	Clad on Base	Thickness (mils)	Phase Shift (deg) 20 KHz	Phase Shift (deg) 200 KHz
		21	10.99	3.88
1	Clad C	42	13.39	4.15
		21	11.02	4.01
2		42	13.47	4.52
		21	10.85	3.92
3		42	13.44	4.45
		21	10.95	4.00
4		42	13.47	4.47
		21	10.96	4.02
5		42	13.57	4.48
		20	15.36	11.79
1	Clad D	40	19.71	11.85
		60	21.00	11.74
		20	15.61	11.70
2		40	19.68	11.74
		60	20.91	11.75
		20	15.35	11.73
3		40	19.62	11.66
		60	20.74	11.78
		20	15.37	11.80
4		40	19.67	11.72
		60	20.96	11.81
		20	15.53	11.74
5		40	19.64	11.95
		60	20.84	11.90

the claddings. The average of the thickness phase shifts was calculated for each cladding. To determine the constants in Equation 11, the following values were first found:

$$S_l = \left(\frac{\Delta P}{\Delta \rho}\right)_l ,$$

$$S_h = \left(\frac{\Delta P}{\Delta \rho}\right)_h ,$$

$$T_l = \left(\frac{\Delta P}{\Delta t}\right)_l , \text{ and}$$

$$T_h = \left(\frac{\Delta P}{\Delta t}\right)_h ,$$

where $(\Delta P/\Delta \rho)_l$ and $(\Delta P/\Delta \rho)_h$ are the changes in phase shifts with respect to resistivity at the low and high frequency, respectively; $(\Delta P/\Delta t)_l$ and $(\Delta P/\Delta t)_h$ are the changes in phase shifts with respect to thickness at the low and high frequency, respectively. For consistency, the phase shifts corresponding to 42 mils (Clad C) and 20 and 40 mils (Clad D) were used in the constant calculation. Thus:

$$S_h = \frac{(11.784 - 4.414)\ \text{deg}}{(9.63 - 15.56)\ \mu\Omega\text{-cm}} = -1.2428\ \text{deg}/\mu\Omega\text{-cm} ,$$

$$S_l = \frac{(19.66 - 13.468)\ \text{deg}}{(9.63 - 15.560)\ \mu\Omega\text{-cm}} = -1.0442\ \text{deg}/\mu\Omega\text{-cm} ,$$

$$T_l = \frac{(15.444 - 19.664)\ \text{deg}}{(20 - 40)\ \text{mils}} = 0.2110\ \text{deg/mil} , \text{ and}$$

$$T_h = \frac{(11.752 - 11.784)\ \text{deg}}{(20-40)\ \text{mils}} = 0.0016\ \text{deg/mil}\ .$$

Therefore:

$$a_{11} = \frac{S_l}{T_h S_l - T_l S_h} = -4.0075\ \text{mil/deg}\ ,$$

$$a_{12} = \frac{S_h}{T_h S_l - T_l S_h} = -4.7697\ \text{mil/deg}\ ,$$

$$a_{21} = \frac{T_l}{T_h S_l - T_l S_h} = 0.0442\ \mu\Omega\text{-cm/deg}\ , \text{and}$$

$$a_{22} = \frac{T_h}{T_h S_l - T_l S_h} = 0.0003\ \mu\Omega\text{-cm/deg}\ .$$

The ratio between constants a_{11} and a_{12} is 0.84.

The measurements were made a second time, but this time with the reference thickness (40 mils) and resistivity (9.63 $\mu\Omega$-cm) phase shifts nulled to zero. The results are given in Table V. The constants (a_{11}, a_{12}, a_{21}, a_{22}) were calculated to be as follows:

$$a_{11} = -1.8748\ \text{mil/deg},$$

$$a_{12} = -2.2038\ \text{mil/deg},$$

$$a_{21} = 0.3859\ \mu\Omega\text{-cm/deg, and}$$

$$a_{22} = 0.0071\ \mu\Omega\text{-cm/deg.}$$

The ratio between constants a_{11} and a_{12} is 0.85. Figures 21 and 22 are plots of phase shifts versus cladding thickness for Clad D at 20 KHz. The curves are approximately linear between 60 and 40 mils; however, they make a hyperbolic cosine approach toward the 20-mil point. Figures 23 and 24 are plots of phase shifts versus cladding thickness for Clad D at 200 KHz. The curves are approximately linear. The latter two figures indicate very little change in phase shift with thickness for the high frequency. This, of course, is in agreement with the basic theory.

By monitoring the phase shift at the two frequencies (20 and 200 KHz) and applying the determined constants to the expression relating phase shift and thickness or resistivity (or conductivity), the thickness of the claddings can be measured independently of the resistivity (or conductivity).

Table V

CLADDING THICKNESS MEASUREMENTS
WITH REFERENCE AT 40 MILS
AND 9.63 MICROHM-CM

Clad	Thickness (mils)	Phase Shift (deg) 20 KHz	200 KHz
C	21	-19.11	-16.44
	42	-13.28	-15.46
	20	- 9.22	- 0.02
D	40	0.00	0.15
	60	2.60	0.32

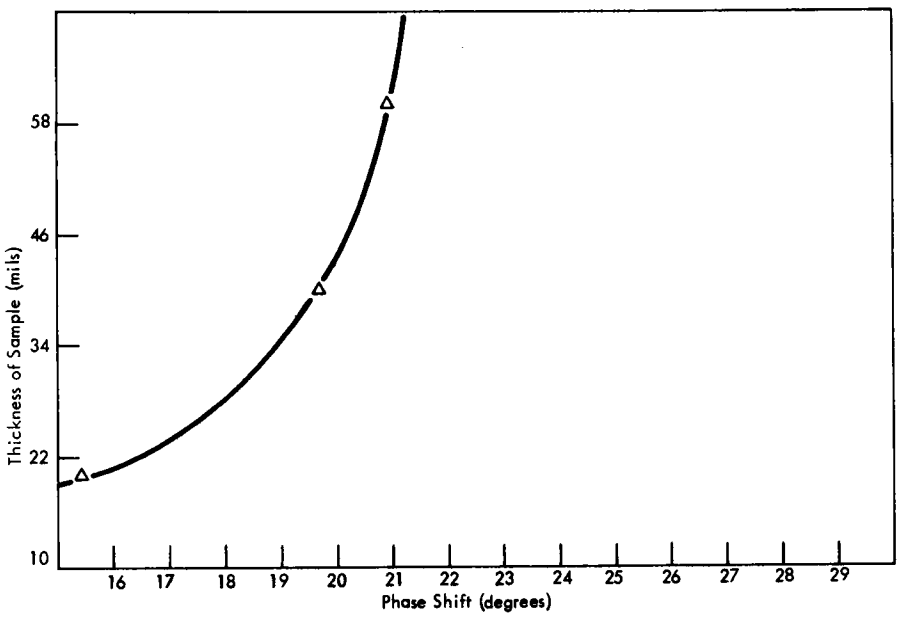


FIGURE 21

THICKNESS VERSUS PHASE SHIFT AT 20 KHz

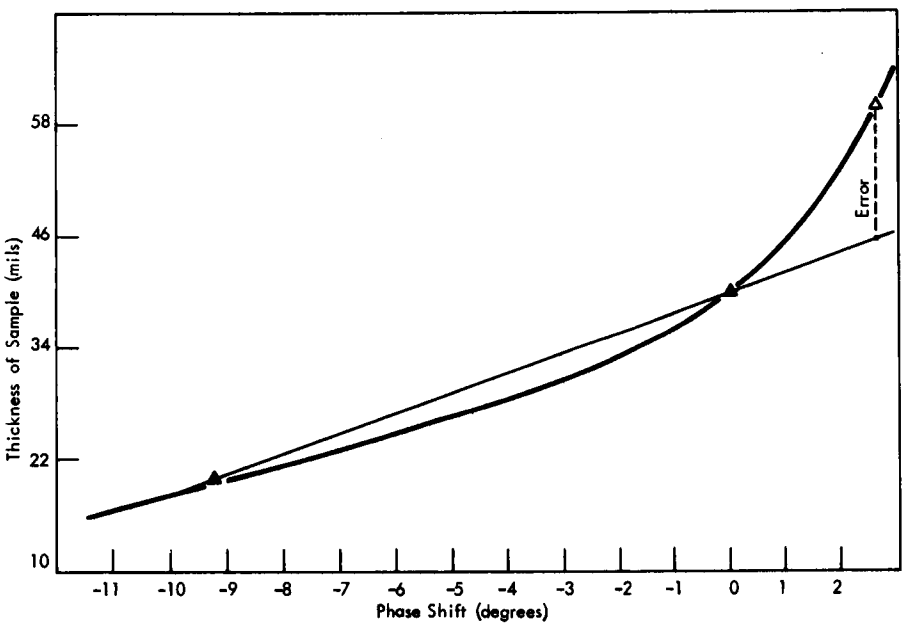


FIGURE 22

THICKNESS VERSUS PHASE SHIFT AT 20 KHz WITH REFERENCE AT 40 MILS

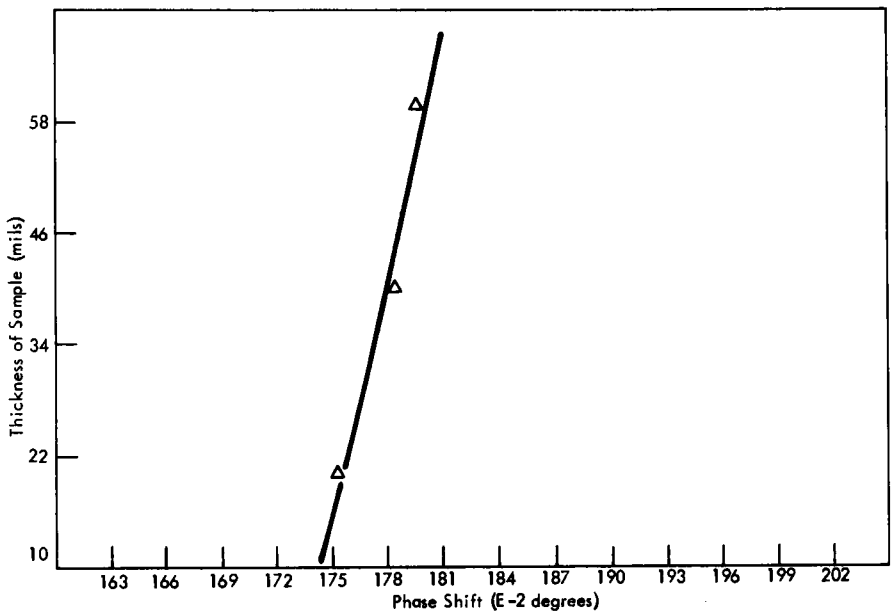


FIGURE 23

THICKNESS VERSUS PHASE SHIFT AT 200 KHz

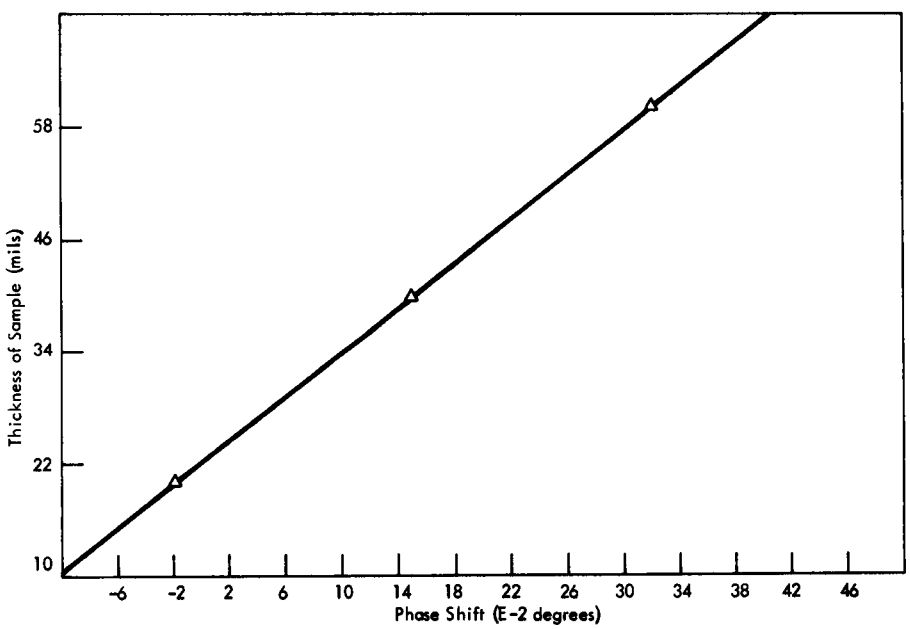


FIGURE 24

THICKNESS VERSUS PHASE SHIFT AT 200 KHz WITH REFERENCE AT 40 MILS

For cladding thickness measurements, Constants a_{11} and a_{12} were dialed on the computer unit. This unit was incorporated into the system by turning the mode-control dial on the digital meter panel to either Comp 1 or Comp 2. The constants become the basic functions for the transformation from phase-shift readings to parameter readings. The phase shifts themselves are considered as input coefficients. Variations in the cladding thickness or resistivity cause the phase shifts or coefficients to vary.

The 40-mil cladding was used as a reference for both thickness and resistivity measurements. In the Comp 1 position, the constant-adjustment dials were varied until the digital panel meter read zero. In the Comp 2 position, the constant-adjustment dials were varied until the digital panel meter read the difference between the resistivities of the two claddings ($\triangle\rho$ = 5.93 $\mu\Omega$-cm). These adjustments, of course, changed the original calculated constants dialed in earlier. The differences between the constants will be discussed later. Since the 40-mil cladding was used as a reference, 40 mils would have to be added to each of the digital panel meter readings to obtain the measured cladding thickness. The value of 9.63 $\mu\Omega$-cm would have to be added to each of the digital panel meter readings to obtain the measured cladding resistivity. As mentioned earlier, the Comp 1 position was used for the thickness measurement and the Comp 2 position for resistivity. Table VI contains the data taken from the two positions. The means and standard deviations are given in Table VII.

Discussion of Errors

One of the most undesirable variables that is encountered in eddy-current measurements is lift off (probe-to-metal spacing). Although this investigation included compensating circuitry for lift off, the actual effect was the minimization of lift off errors and not their elimination. The lift-off range was chosen to be small, thus lessening the lift off effect.

Table VI

THICKNESS AND RESISTIVITY USING COMPUTER UNIT

Clad D (9.63 microhm-cm)					Clad C (15.56 microhm-cm)			
Measurement Number	Instrument Reading for				Measurement Number	Instrument Reading for		
	20 Mils	40 Mils	60 Mils	Conductivity		21 Mils	42 Mils	Conductivity
1	-20.22	-01.11	+03.65	+00.05	1	-08.99	+02.06	+06.08
2	-20.65	-01.42	+03.76	+00.08	2	-09.02	+02.70	+05.85
3	-19.96	+00.04	+03.99	+00.72	3	-10.74	+02.30	+06.02
4	-19.95	+00.19	+04.78	+00.58	4	-10.40	+02.49	+06.14
5	-20.07	-00.26	+04.44	+00.60	5	-10.78	+02.50	+05.96
6	-20.00	+00.16	+04.44	+00.56	6	-10.62	+03.24	+06.07
7	-19.38	-00.08	+04.71	+00.50	7	-11.00	+01.96	+05.99
8	-19.40	+00.26	+05.02	+00.60	8	-10.48	+03.25	+06.06
9	-20.20	-00.03	+04.06	+00.47	9	-09.33	+01.44	+06.02
10	-19.98	-00.10	+05.16	+00.51	10	-12.95	+02.45	+06.23
11	-20.47	-00.33	+04.84	+00.46	11	-12.59	+02.50	+06.20
12	-19.95	+00.08	+05.42	+00.52	12	-09.15	+00.45	+06.15
13	-19.87	+00.10	+05.36	+00.54	13	-09.34	+01.80	+05.99

Table VII

SUMMARY OF THICKNESS AND RESISTIVITY MEASUREMENTS USING THE COMPUTER UNIT

Actual Thickness (mils)	Mean and Standard Deviation of the Measured Thickness (mils)	Percent Deviation between the Actual and Measured Thickness	Actual Resistivity (microhm-cm)	Mean and Standard Deviation of the Measured Resistivity (microhm cm)	Percent Deviation between the Actual and Measured Resistivity
20	19.990 ± 0.356	0.05			
40	39.807 ± 0.509	0.05	9.630	10.106 ± 0.195	5.00
60	44.589 ± 0.589	25.68			
21	29.585 ± 1.281	40.88	15.560	15.688 ± 0.826	0.83
42	42.241 ± 0.743	0.56			

However, the cladding thickness measurement range was approximately a 33% variation. The lift-off effect increases as the range of measurements increases.

One other source of error was the stacking of the claddings to vary the thickness. Two and three 20-mil layers of Clad C were used to obtain thicknesses of 40 and 60 mils, respectively. This arrangement, of course, meant having layers of air between the claddings. The amount of error encountered due to the air gaps could not be determined.

Coil-temperature variations produced as a result of handling the probe coil can affect the readings. Temperature variation causes undesirable drift in the eddy-current system, thus resulting in error.

Still one other source of error was the drift in the system due to the input power fluctuation. However, this effect seemed to be quite small.

The latter two sources of error also played a major role in determining the constants for the computer unit. System drifts due to power fluctuations and temperature variations caused the input coefficients or phase shifts to vary, thus causing a change in the constant settings. Approximately 24 hours elapsed between the determination of the constants and the cladding thickness measurements. The percent deviations between the calculated constants for the thickness measurement and the set used were approximately 13 and 14% for a_{11} and a_{12}, respectively.

Conclusions

This investigation has shown that cladding thicknesses can be measured with a dual-frequency eddy-current system with an accuracy greater than 99%. The thickness range measured in this investigation was much greater than the 10% linear range. Nevertheless, the sample thicknesses used to determine the computer constants were experimentally determined to within 1%. However, due to the nonlinearity, the points that fell between 20

and 40 mils (see Figure 22, Page 37) exhibit deviations from zero to a maximum of approximately 3 mils. This maximum occurs at approximately 30 mils on the straight line on Figure 22. Also, due to nonlinearity, the points above 40 mils and below 20 mils exhibit progressive deviations.

The portion of the experimental curve between 40 and 60 mils appears quite linear (see Figure 22). Had sample thicknesses been measured in this range, the deviations would have been quite small compared to the 20 to 40-mil range. The former range fits the thickness-phase shift relation in Equation 7 better than the latter range.

BIBLIOGRAPHY

BIBLIOGRAPHY

Dodd, C. V., Basic Principles of Eddy-Current Testing (March 27, 1972).

Dodd, C. V., Cheng, C. C., Simpson, W. A., Deeds, D. A., and Smith, J. H., The Analysis of Reflection Type Coils for Eddy-Current Testing, ORNL-TM-4107 (April 1973).

Libby, H. L.; Introduction to Electromagnetic Nondestructive Test Methods, (Wiley-Interscience, a Division of John Wiley and Sons, Inc, New York, 1971).

APPENDICES

APPENDIX A

COMPUTER PROGRAM FOR PROCESSING

EDDY-CURRENT DATA

```
10 DIM X[20,20],Y[20],Z[20]
20 PRINT LIN4
30 PRINT TAB24"EDDY CURRENT PLOT FOR J.T.HILL"
40 PRINT LIN3
50 DISP "LOAD PLOTTER PAPER,CONT";
60 STOP
70 DISP "X-MIN FOR PLOT=";
80 INPUT X1
90 DISP "X-MAX FOR PLOT=";
100 INPUT X2
110 DISP "NO OF X DIVISIONS=";
120 INPUT X3
130 DISP "Y-MIN FOR PLOT=";
140 INPUT Y1
150 DISP "Y-MAX FOR PLOT=";
160 INPUT Y2
170 DISP "NO. OF Y DIVISIONS=";
180 INPUT Y3
190 X4=(X2-X1)/X3
200 Y4=(Y2-Y1)/Y3
210 SCALE X1,X2,Y1,Y2
220 XAXIS Y1,X4
230 YAXIS X1,Y4
240 PLOT X2,Y1
250 PLOT X2,Y2
260 PLOT X1,Y2,-1
270 BEEP
280 DISP "MOVE PEN DOWN APPROX 1/2 Y DIV";
290 STOP
300 LABEL (310,1.3,1.7,0,8.5/11)
310 FORMAT 3F4.0
320 FOR X=X1+X4 TO X2-X4 STEP X4
330 PLOT X,Y1,1
340 CPLOT -2,3
350 LABEL (310)X
360 NEXT X
370 PLOT 5*X4+X1,Y1
380 LABEL (*,2,1.7,0,8.5/11)"PHASE SHIFT (DEGREES) --->"
390 BEEP
400 DISP "RETURN PEN TO ORIG. ORIGIN"
410 WAIT 2000
420 BEEP
430 DISP "MOVE PEN OVER APPROX 1/2 X DIV";
440 STOP
450 LABEL (*,1.3,1.7,0,8.5/11)
460 FOR Y=Y1 TO (Y2-Y4) STEP Y4
470 PLOT X1,Y,1
480 CPLOT 3,-0.03
490 LABEL (310,1.3,1.7,0,8.5/11)Y
500 NEXT Y
510 PLOT X1+0.2*X4,Y1+Y4
520 DEG
```

```
530 LABEL (*,2,1.7,90,8.5/11)"RESISTIVITY (MICRO-OHM CM) --->"
540 BEEP
550 DISP "RETURN PEN TO ORIG. ORIGIN";
560 STOP
570 PRINT TAB32"STANDARD VALUES"
580 PRINT LIN2
590 PRINT TAB7"RESISTIVITY";TAB24"AVERAGE";TAB40"STANDARD";
600 PRINT TAB50"95 PERCENT"
610 PRINT TAB6"(MICRO-OHM CM)";TAB25"PHASE";TAB40"DEVIATION";
620 PRINT TAB50"CONFIDENCE"
630 PRINT TAB25"SHIFT";TAB53 "LIMITS"
640 PRINT LIN3
650 S1=S2=S3=S4=S5=S6=S7=T7=T8=0
660 DISP "NO. OF STD RESISTIVITIES=";
670 INPUT M
680 FOR I=1 TO M
690 S1=S2=0
700 FIXED 0
710 DISP "RESISTIVITY FOR STD NO.";I;"=";
720 INPUT Y[I]
730 DISP "NO. PHASE SHIFTS FOR STD NO.";I;"=";
740 INPUT N
750 Z[I]=0
760 FOR J=1 TO N
770 DISP "PHASE SHIFT FOR PT NO";J;"=";
780 INPUT X[I,J]
790 S1=X[I,J]+S1
800 S2=X[I,J]↑2+S2
810 NEXT J
820 S3=S4=S5=S6=S7=0
830 Z[I]=S1/N
840 S=SQR((N*S2-S1*S1)/(N*(N-1)))
850 R=(1.96*S)/(SQRN)
860 FIXED 5
870 PRINT TAB7,Y[I];TAB23,Z[I];TAB40,S;TAB60,R
880 PRINT
890 PLOT Z[I],Y[I],-1
900 PLOT Z[I],Y[I]+Y4/20
910 PLOT Z[I]+X4/10,Y[I]-Y4/20
920 PLOT Z[I]-X4/10,Y[I]-Y4/20
930 PLOT Z[I],Y[I]+Y4/20
940 PEN
950 NEXT I
960 FOR I=1 TO M
970 T7=T7+Z[I]
980 T8=T8+Z[I]↑2
990 S3=S3+Z[I]↑3
1000 S4=S4+Z[I]↑4
1010 S5=S5+Y[I]
1020 S6=S6+Z[I]*Y[I]
1030 S7=S7+Z[I]↑2*Y[I]
1040 NEXT I
1050 PRINT LIN4
1060 PRINT TAB27"SECOND ORDER LEAST SQUARES"
1070 PRINT TAB32"FIT COEFFICIENTS"
1080 PRINT LIN3
1090 T1=M*(T8*S4-S3*S3)
1100 T2=T7*(T7*S4-T8*S3)
1110 T3=T8*(T7*S3-T8*T8)
1120 T4=T1-T2+T3
1130 T1=M*(T8*S7-S3*S6)
1140 T2=T7*(T7*S7-T8*S6)
1150 T3=S5*(T7*S3-T8*T8)
1160 A3=(T1-T2+T3)/T4
1170 T5=S6-A3*S3
```

```
1180 T6=S5-A3*T8
1190 A1=(T6*T8-T5*T7)/(M*T8-T7*T7)
1200 A2=(M*T5-T6*T7)/(M*T8-T7*T7)
1210 FLOAT 9
1220 PRINT TAB20"A0= ";A1
1230 PRINT
1240 PRINT TAB20"A1",A2
1250 PRINT
1260 PRINT TAB20"A2",A3
1270 PRINT LIN4
1280 FOR X=X1 TO X2 STEP X4/10
1290 Y=A1+A2*X+A3*X↑2
1300 IF Y<Y1 THEN 1330
1310 IF Y>Y2 THEN 1330
1320 PLOT X,Y
1330 NEXT X
1340 PEN
1350 DISP "CHANGE PEN COLOR";
1360 STOP
1370 PRINT TAB34"PART VALUES"
1380 PRINT LIN3
1390 PRINT TAB6"AVERAGE";TAB20"STANDARD";TAB39"95 PERCENT";
1400 PRINT TAB60"CALCULATED"
1410 PRINT TAB7"PHASE";TAB20"DEVIATION";TAB39"CONFIDENCE";TAB60"RESISTIVITY"
1420 PRINT TAB7"SHIFT";TAB41"LIMITS";TAB58"(MICRO-OHM CM)"
1430 PRINT LIN3
1440 S1=S2=S3=S4=0
1450 DISP "NO. SAMPLES CHECKED=";
1460 INPUT M
1470 FOR I=1 TO M
1480 S1=S2=0
1490 FIXED 0
1500 DISP "NO. PHASE SHIFTS FOR PT NO.";I;"=";
1510 INPUT N
1520 FOR J=1 TO N
1530 DISP "PHASE SHIFT FOR PT NO";J;"=";
1540 INPUT X
1550 S1=S1+X
1560 S2=S2+X↑2
1570 NEXT J
1580 X=S1/N
1590 S=SQR((N*S2-S1*S1)/(N*(N-1)))
1600 R=1.96*S/SQRN
1610 Y=A1+A2*X+A3*X↑2
1620 FIXED 5
1630 PRINT TAB8,X;TAB22,S;TAB40,R;TAB62,Y
1640 PRINT
1650 PLOT X,Y,-1
1660 PLOT X,Y+Y4/20
1670 PLOT X+X4/10,Y-Y4/20
1680 PLOT X-X4/10,Y-Y4/20
1690 PLOT X,Y+Y4/20
1700 PEN
1710 NEXT I
1720 PRINT LIN10
1730 END
```

APPENDIX B

This program calculates the magnitude and phase of the voltage that is fed to the phase-measuring circuits of the phase-sensitive eddy-current instrument, and is designed to help analyze eddy-current measurements of cladding thickness. The input data for the program is contained in Lines 250 through 520. The data are inputted as follows:

00250	R5	= (coil mean radius in inches)
00260	R1	= (normalized inner radius of driver coil)
00270	R2	= (normalized outer radius of driver coil)
00280	L3	= (normalized length of driver coil)
00290	R3	= (normalized inner radius of pickup coil)
00300	R4	= (normalized outer radius of pickup coil)
00310	L4	= (normalized length of pickup coil)
00320	L5	= (normalized length of recess of each pickup coil from the face of the driver coil)
00330	L6	= (normalized minimum lift off of the driver coil)
00340	R6	= (resistance of driver coil in ohms)
00350	R7	= (resistance of both pickup coils in ohms)
00360	N3	= (number of turns on the driver coil)
00370	N4	= (number of turns on each pickup coil)
00380	R0	= (driver amplifier series resistance in ohms)
00390	R9	= (pickup amplifier shunt resistance in ohms)
00400	C6	= (shunt capacitance of driver circuit in farads)
00410	C7	= (shunt capacitance of pickup circuit in farads)
00420	V0	= (output voltage in volts)

00430 GAIN = (amplifier gain)

00440 FREQ = (operating frequency in Hertz)

00450 L2 = (normalized lift-off increment of the driver coil)

00460 RH01 = (resistivity of base material in microhm-cm)

00470 U1 = (relative magnetic permeability of base material)

00480 RH02 = (resistivity of cladding material in microhm-cm)

00490 U2 = (relative magnetic permeability of cladding material)

00500 CLAD(1) = (numerical value of minimum cladding thickness in inches)

00510 CLAD(2) = (numerical value of nominal cladding thickness in inches)

00520 CLAD(3) = (numerical value of maximum cladding thickness in inches)

```
00010C IN THIS PRØGRAM, THE BASE RESISTIVITY IS RH01 AND
00020C   THE CLADDING RESISTIVITY IS RH02
00030C SIGMA IS THE GAMMA FACTØR
00040      CØMPLEX BETA1,BETA2,EX1,RNUM,DEN,SIGMA
00050      CØMPLEX TMUT,DRIVER,PICKUP
00060      REAL L3,L4,L5,L6,L2,N3,N4,K1,K2
00070      CØMMØN X,Z,Q1,PI/B1/R1,R2,R3,R4,L3,L4,R0,R6,R7
00080      CØMMØN /B1/R9,C6,C7,V0,GAIN,W,FREQ,R5,N3,N4
00090      CØMMØN /B2/TMUT,DRIVER,PICKUP,AIR1,AIR2/B3/GAGE,XIN
00100      CØMMØN /B3/X0UT,XLEN,TURNS,N1A,J1,PERLAY,XCAY
00110      DIMENSIØN CLAD(3),RL(5),SIGMA(3),TMUT(3,5),DRIVER(3,5)
00120      DIMENSIØN PICKUP(3,5),TMAG(3,5),PHASE(3,5),SHIFT(3,5)
00130      EQUIVALENCE (RH01,K1),(RH02,K2),(GAIN,G5),(FREQ,F)
00140      PI=3.14159265
00150      RAD=180.0/PI
00160C
00170C
00180C
00190C
00200C
00210C
00220      JKL=0
00230C THE FØLLØWING ARE INPUT DATA FØR THE PARAMETERS ØF
00240C   THE CØILS,MATERIAL, AND CIRCUIT
00250      R5=.08325
00260      R1=.75
00270      R2=1.25
00280      L3=.36
00290      R3=.36
00300      R4=.696
00310      L4=.096
00320      L5=0.0
00330      L6=.1
00340      R6=79.36
00350      R7=530.5
00360      N3=360.0
00370      N4=410.0
00380      R0=1.0E6
00390      R9=1.0E6
00400      C6=1.0E-12
00410      C7=1.0E-12
00420      V0=10.0
00430      GAIN=1.0
00440      FREQ=1.0E4
00450      L2=0.025
00460      RH01=5.393
00470      U1=1.0
00480      RH02=3.632
00490      U2=1.0
00500      CLAD(1)=0.0266
00510      CLAD(2)=0.028
00520      CLAD(3)=0.0294
00530    5 W=2.0*PI*FREQ
00540      IF(RH01.GT.1.0E9) GØ TØ 10
00550      RM1=0.5094*U1*FREQ*R5*R5/RH01
00560      GØ TØ 20
00570   10 RM1=0.0
00580   20 RM2=0.5094*U2*FREQ*R5*R5/RH02
00590C THE SYSTEM PARAMETERS ARE PRINTED ØUT
```

```
00600       IF(JKL.NE.0) GØ TØ 105
00610       TYPE 30,R1,R2,L3
00620    30 FØRMAT(1H ,3HR1=,F8.5,3X,3HR2=,F8.5,3X,14HDRIVER LENGTH=,
00630      1F8.5)
00640       TYPE 40,R3,R4,L4
00650    40 FØRMAT(1H ,3HR3=,F8.5,3X,3HR4=,F8.5,3X,14HPICKUP LENGTH=,
00660      1F8.5)
00670       TYPE 50,R5,FREQ
00680    50 FØRMAT(1H ,17HCØIL MEAN RADIUS=,F8.5,7H INCHES,3X,
00690      120HØPERATING FREQUENCY=,1PE12.5)
00700       TYPE 60,L5
00710    60 FØRMAT(1H ,15HPICKUP RECESSED,F8.5)
00720       TYPE 70,L6,L2
00730    70 FØRMAT(1H ,13HMIN LIFT-ØFF=,F8.5,3X,19HLIFT-ØFF INCREMENT=,
00740      1F8.5)
00750       TYPE 80,U1,RM1,RHØ1
00760    80 FØRMAT(1H ,3HU1=,F6.2,5X,3HM1=,F9.5,2X,12HRESISTIVITY=,
00770      11PE12.5,11H MICRØHM CM)
00780       TYPE 90,U2,RM2,RHØ2
00790    90 FØRMAT(1H ,3HU2=,F6.2,5X,3HM2=,F9.5,2X,12HRESISTIVITY=,
00800      11PE12.5,11H MICRØHM CM)
00810       TYPE 100,CLAD(1),CLAD(2),CLAD(3)
00820   100 FØRMAT(1H ,10HTHICKNESS=,F8.5,2(8X,F8.5))
00830C THE INTEGRATIØN IS PERFØRMED BY THE TRAPEZØIDAL METHØD,
00840C   EVALUATING AT THE CENTER ØF THE INTERVAL; FØR X LARGE
00850C   THE INTEGRAL CØNVERGES RAPIDLY,SØ LARGER INTERVALS
00860C   ARE TAKEN
00870C IN THE INTEGRATIØN TMUT, DRIVER, PICKUP, AIR1, AND
00880C   AIR2 ARE CALCULATED
00890   105 S1=0.01
00900       S2=5.0
00910       B1=0.0
00920       B2=S2
00930       AIR1=0.0
00940       AIR2=0.0
00950       DØ 108 J=1,3
00960       DØ 108 K=1,5
00970       DRIVER(J,K)=(0.0,0.0)
00980       PICKUP(J,K)=(0.0,0.0)
00990       TMUT(J,K)=(0.0,0.0)
01000   108 CØNTINUE
01010   110 I1=(B2-B1)/S1
01020       X=B1-S1/2.0
01030       DØ 170 I=1,I1
01040       X=X+S1
01050       Z=R2*X
01060       Q1=R2
01070C SUBRØUTINE BESSEL EVALUATES THE INTEGRAL ØF
01080C   THE PRØDUCT ØF THE BESSEL FUNCTIØN AND ITS
01090C   ARGUMENT
01100       CALL BESSEL(VAL2)
01110       Z=R1*X
01120       Q1=R1
01130       CALL BESSEL(VAL1)
01140       Z=R4*X
01150       Q1=R4
01160       CALL BESSEL(VAL4)
01170       Z=R3*X
01180       Q1=R3
```

```
01190       CALL BESSEL(VAL3)
01200       S3=S1*(VAL4-VAL3)*(VAL2-VAL1)
01210       S4=S1*(VAL2-VAL1)*(VAL2-VAL1)
01220       S5=S1*(VAL4-VAL3)*(VAL4-VAL3)
01230       EX3=EXP(-X*L3)
01240       W1=1.0-EX3
01250       EX4=EXP(-X*L4)
01260       W2=1.0-EX4
01270       EX5=EXP(-X*L5)
01280       W3=EX3/(EX4*EX4*EX5*EX5)
01290       IF(X.GT.30.0) GØ TØ 160
01300C FRØM HERE THRØUGH LINE 130,SIGMA IS CALCULATED
01310       BETA2=CSQRT(CMPLX(X*X,RM2))/U2
01320       DØ 130 J=1,3
01330       IF(REAL(CLAD(J)/R5*BETA2*U2).GT.15.0) GØ TØ 120
01340       EX1=CEXP(2.0*CLAD(J)/R5*BETA2*U2)
01350       BETA1=CSQRT(CMPLX(X*X,RM1))/U1
01360       RNUM=(X+BETA2)*(BETA2-BETA1)+(X-BETA2)*(BETA2+BETA1)*EX1
01370       DEN=(X-BETA2)*(BETA2-BETA1)+(X+BETA2)*(BETA2+BETA1)*EX1
01380       SIGMA(J)=RNUM/DEN
01390       GØ TØ 130
01400   120 SIGMA(J)=(X-BETA2)/(X+BETA2)
01410   130 CØNTINUE
01420       EX2=EXP(-2.0*X*L2)
01430       EX6=EXP(-2.0*X*L6)
01440       W4=1.0-EX4*W3
01450       W5=EX5*EX6*W1*W2*W4
01460       W6=EX6*W1*W1
01470       W7=W2*W2*EX6*EX5*EX5*W4*W4
01480       RL(1)=1.0
01490       DØ 140 K=2,5
01500   140 RL(K)=EX2*RL(K-1)
01510       DØ 150 K=1,3
01520       DØ 150 L=1,5
01530       TMUT(K,L)=TMUT(K,L)+S3*W5*RL(L)*SIGMA(K)
01540       DRIVER(K,L)=DRIVER(K,L)+S4*W6*RL(L)*SIGMA(K)
01550   150 PICKUP(K,L)=PICKUP(K,L)+S5*W7*RL(L)*SIGMA(K)
01560   160 AIR1=AIR1+S4*2.0*(X*L3-W1)
01570       AIR2=AIR2+S5*(4.0*(X*L4-W2)-2.0*W2*W2*W3)
01580   170 CØNTINUE
01590       B1=B2
01600       B2=B2+S2
01610       S1=0.05
01620       IF(X.LT.9.0) GØ TØ 110
01630       S1=0.1
01640       IF(X.LT.29.0) GØ TØ 110
01650       S1=0.2
01660       IF(X.LT.39.0) GØ TØ 110
01670       S1=0.5
01680       IF(X.LT.79.0) GØ TØ 110
01690C THE INTEGRATIØN ENDS HERE
01700       IF(JKL.NE.0) GØ TØ 552
01710C NEXT THE PRØPERTIES ØF THE CØILS ARE DETERMINED AND PRINTED
01720   180 CALL CIRCT(TMAG,PHASE,QO,T1,T2)
01730       CALL PHASET(TMAG,PHASE,SHIFT,V1,SET)
01740       TYPE 190
01750   190 FØRMAT(1H ,10HDRIVER RES,4X,10HINDUCTANCE,4X,8HNØ TURNS,
01760      16X,9HSHUNT CAP,5X,9HNØR IM PT)
01770       Q1=QO*T1*T1*AIR1/W
```

```
01780       Q2=(REAL(DRIVER(2,3))+AIR1)/AIR1
01790       Q3=Q0*T2*T2*AIR2/W
01800       Q4=(REAL(PICKUP(2,3))+AIR2)/AIR2
01810       TYPE 200,R6,Q1,N3,C6,Q2
01820   200 F0RMAT(1H ,1PE12.5,2X,1PE12.5,2X,0PF8.1,6X,1PE12.5,2X,
01830      10PF9.6)
01840       TYPE 210
01850   210 F0RMAT(1H ,10HPICKUP RES,4X,10HINDUCTANCE,4X,8HN0 TURNS,
01860      16X,9HSHUNT CAP,5X,9HN0R IM PT)
01870       TYPE 200,R7,Q3,N4,C7,Q4
01880       TYPE 220
01890   220 F0RMAT(1H ,12HDRIVING V0LT,2X,10HSERIES RES,4X,
01900      18HAMP GAIN,6X,9HINPUT IMP)
01910       TYPE 230,V0,R0,GAIN,R9
01920   230 F0RMAT(1H ,F5.1,9X,1PE12.5,2X,0PF8.1,6X,1PE12.5)
01930       TYPE 240,V1
01940   240 F0RMAT(1H ,22HDISCRIMINAT0R V0LTAGE=,1PE12.5)
01950       TYPE 250
01960   250 F0RMAT(1H )
01970       RL(1)=L6
01980       D0 260 I=2,5
01990   260 RL(I)=L2+RL(I-1)
02000       TYPE 270,RL
02010   270 F0RMAT(1H ,4(F6.3,8X),F6.3)
02020       TYPE 250
02030C  THE V0LTAGE MAGNITUDE,PHASE,AND SHIFT ARE PRINTED F0R
02040C    THE VARI0US LIFT-0FF VALUES
02050       D0 280 I=1,3
02060       TYPE 290,(TMAG(I,J),J=1,5)
02070       TYPE 290,(PHASE(I,J),J=1,5)
02080       TYPE 290,(SHIFT(I,J),J=1,5)
02090       TYPE 250
02100   280 C0NTINUE
02110   290 F0RMAT(1H ,4(1PE12.5,2X),1PE12.5)
02120       CALL SENS(SHIFT,RAD,SEN)
02130C  THE USER SELECTS 0NE 0F F0UR P0SSIBILITIES
02140   295 TYPE 300
02150   300 F0RMAT(' 1 C0IL DESIGN  2 ATTEN. DESIGN  3 DRIFT CHECK
02160      1  4 C0N CAL')
02170       TYPE 250
02180       ACCEPT 310,N5
02190   310 F0RMAT(I1)
02200       G0 T0(320,450,540,690),N5
02210C  THE FIRST P0SSIBILITY PRINTS FACT0RS IN THE  C0IL
02220C    DESIGN; USER INPUTS INTEGER DATA AS REQUESTED
02230   320 TYPE 330
02240   330 F0RMAT(' DRIVER WIRE GAGE, TURNS, PICKUP WIRE GAGE,
02250      1 TURNS')
02260       TYPE 250
02270       ACCEPT 340,N1A,N2A,N3A,N4A
02280   340 F0RMAT(4I)
02290       IF (N1A*N2A.EQ.0) G0 T0 350
02300       GAGE=N1A
02310       XIN=R1*R5
02320       X0UT=R2*R5
02330       XLEN=L3*R5
02340       TURNS=N2A
02350       N3=N2A
02360       N1A=-1
```

```
02370       J1=1
02380       CALL GAGER(R6)
02390       GØ TØ 370
02400   350 IF(N1A.EQ.0) GØ TØ 360
02410       GAGE=N1A
02420       XIN=R1*R5
02430       XØUT=R2*R5
02440       XLEN=L3*R5
02450       J1=1
02460       CALL GAGER(R6)
02470       N3=TURNS
02480       GØ TØ 370
02490   360 IF(N2A.EQ.0) GØ TØ 390
02500       N3=N2A
02510       TURNS=N2A
02520       XIN=R1*R5
02530       XØUT=R2*R5
02540       XLEN=L3*R5
02550       J1=0
02560       CALL GAGER(R6)
02570   370 TYPE 380,TURNS,GAGE,PERLAY,XLAY,R6
02580   380 FØRMAT(1H ,6HDRIVER,F6.1,10H TURNS ØF#,F5.1,4HWIRE,
02590      1F5.1,6H/LAYER,F5.1,6HLAYERS,1PE12.5,4HØHMS)
02600   390 IF(N3A*N4A.EQ.0) GØ TØ 400
02610       GAGE=N3A
02620       TURNS=N4A
02630       N4=N4A
02640       XIN=R3*R5
02650       XØUT=R4*R5
02660       XLEN=L4*R5
02670       J1=1
02680       CALL GAGER(R7)
02690       R7=2.0*R7
02700       GØ TØ 420
02710   400 IF(N3A.EQ.0) GØ TØ 410
02720       GAGE=N3A
02730       XIN=R3*R5
02740       XØUT=R4*R5
02750       XLEN=L4*R5
02760       J1=1
02770       CALL GAGER(R7)
02780       N4=TURNS
02790       R7=2.0*R7
02800       GØ TØ 420
02810   410 IF(N4A.EQ.0) GØ TØ 440
02820       N4=N4A
02830       TURNS=N4A
02840       XIN=R3*R5
02850       XØUT=R4*R5
02860       XLEN=L4*R5
02870       J1=0
02880       CALL GAGER(R7)
02890       R7=2.0*R7
02900   420 TYPE 430,TURNS,GAGE,PERLAY,XLAY,R7
02910   430 FØRMAT(1H ,6HPICKUP,F6.1,10H TURNS EA#,F5.1,4HWIRE,
02920      1F5.1,6H/LAYER,F5.1,6HLAYERS,1PE12.5,4HØHMS)
02930   440 GØ TØ 180
02940C THE SECØND PØSSIBILITY DEALS WITH ATTENUATØR DESIGN;
```

```
02950C   USER INPUTS REQUESTED DATA IN E FIELD TYPE
02960   450 TYPE 460
02970   460 FØRMAT(' DRIVER SERIES RES, SHUNT CAP, PICKUP SHUNT RES,
02980      1 SHUNT CAP')
02990       TYPE 250
03000       ACCEPT 470,P1,P2,P3,P4
03010   470 FØRMAT(4E)
03020       IF(P1.EQ.0.0) GØ TØ 480
03030       RO=P1
03040   480 IF(P2.EQ.0.0) GØ TØ 490
03050       C6=P2
03060   490 IF(P3.EQ.0.0) GØ TØ 500
03070       R9=P3
03080   500 IF(P4.EQ.0.0) GØ TØ 510
03090       C7=P4
03100   510 Q5=1.0/(W*SQRT(Q1*Q2*C6))
03110       Q6=SQRT(Q1*Q2/C6)
03120       Q7=RO/(W*Q1*Q2)
03130       Q8=1.0/(W*SQRT(Q3*Q4*C7))
03140       Q9=SQRT(Q3*Q4/C7)
03150       Q10=R9/(W*Q3*Q4)
03160       TYPE 520,Q5,Q6,Q7
03170   520 FØRMAT(1H ,7HDVR CKT,1PE12.5,10H BELØW RES,1PE12.5,
03180      18H ØPT RES,1PE12.5,11H RES/REACT.)
03190       TYPE 530,Q8,Q9,Q10
03200   530 FØRMAT(1H ,7HP-U CKT,1PE12.5,10H BELow RES,1PE12.5,
03210      18H ØPT RES,1PE12.5,11H RES/REACT.)
03220       GØ TØ 180
03230C THE THIRD PØSSIBILITY EXAMINES THE EFFECTS ØF DRIFT
03240C   ØN THE SYSTEM
03250   540 TYPE 550
03260   550 FØRMAT(1H ,23HSYSTEM DRIFT VARIATIØNS)
03270       DR1=0.01
03280       DR2=0.01
03290       DR3=0.01
03300       DR4=0.01
03310       DR5=0.01
03320       DR6=0.01
03330       DR7=0.01
03340       DR8=0.01
03350       DR9=0.01
03360       DR10=0.01
03370       DR11=0.01
03380       GØ TØ 559
03390   552 CALL CIRCT1(SET,V1,SHIFT,RAD,SEN)
03400       GØ TØ (675,678,681,684),JKL
03410   559 TYPE 560
03420   560 FØRMAT(1H ,11H% VARIATIØN,3X,13HPARAMETER VAR,1X,
03430      17HRADIANS,7X,7HDEGREES,7X,10H% ØF RANGE)
03440       IF(DR1.EQ.0.0) GØ TØ 580
03450       R6=R6*(1.0+DR1)
03460       DR100=100.0*DR1
03470       TYPE 570,DR100
03480   570 FØRMAT(1H ,F4.1,10X,13HDRIVER RES    $)
03490       CALL CIRCT1(SET,V1,SHIFT,RAD,SEN)
03500       R6=R6/(1.0+DR1)
03510   580 IF(DR2.EQ.0.0) GØ TØ 600
03520       R7=R7*(1.0+DR2)
03530       DR100=100.0*DR2
```

```
03540       TYPE 590,DR100
03550   590 FØRMAT(1H ,F4.1,10X,13HPICKUP RES    $)
03560       CALL CIRCT1(SET,V1,SHIFT,RAD,SEN)
03570       R7=R7/(1.0+DR2)
03580   600 IF(DR3.EQ.0.0) GØ TØ 620
03590       C6=C6*(1.0+DR3)
03600       DR100=100.0*DR3
03610       TYPE 610,DR100
03620   610 FØRMAT(1H ,F4.1,10X,13HDVR SHUNT CAP$)
03630       CALL CIRCT1(SET,V1,SHIFT,RAD,SEN)
03640       C6=C6/(1.0+DR3)
03650   620 IF(DR4.EQ.0.0) GØ TØ 640
03660       C7=C7*(1.0+DR4)
03670       DR100=100.0*DR4
03680       TYPE 630,DR100
03690   630 FØRMAT(1H ,F4.1,10X,13HP-U SHUNT CAP$)
03700       CALL CIRCT1(SET,V1,SHIFT,RAD,SEN)
03710       C7=C7/(1.0+DR4)
03720   640 IF(DR5.EQ.0.0) GØ TØ 660
03730       RO=RO*(1.0+DR5)
03740       DR100=100.0*DR5
03750       TYPE 650,DR100
03760   650 FØRMAT(1H ,F4.1,10X,13HSERIES RES    $)
03770       CALL CIRCT1(SET,V1,SHIFT,RAD,SEN)
03780       RO=RO/(1.0+DR5)
03790   660 IF(DR6.EQ.0.0) GØ TØ 671
03800       R9=R9*(1.0+DR6)
03810       DR100=100.0*DR6
03820       TYPE 670,DR100
03830   670 FØRMAT(1H ,F4.1,10X,13HAMP INPUT RES$)
03840       CALL CIRCT1(SET,V1,SHIFT,RAD,SEN)
03850       R9=R9/(1.0+DR6)
03860   671 IF(DR7.EQ.0.0) GØ TØ 673
03870       VO=VO*(1.0+DR7)
03880       DR100=100.0*DR7
03890       TYPE 672,DR100
03900   672 FØRMAT(1H ,F4.1,10X,13HAPPLIED VØLT.$)
03910       CALL CIRCT1(SET,V1,SHIFT,RAD,SEN)
03920       VO=VO/(1.0+DR7)
03930   673 IF(DR8.EQ.0.0) GØ TØ 676
03940       FREQ=FREQ*(1.0+DR8)
03950       DR100=100.0*DR8
03960       TYPE 674,DR100
03970   674 FØRMAT(1H ,F4.1,10X,13HFREQUENCY     $)
03980       JKL=1
03990       GØ TØ 5
04000   675 FREQ=FREQ/(1.0+DR8)
04010       JKL=0
04020   676 IF(DR9.EQ.0.0) GØ TØ 679
04030       R5=R5*(1.0+DR9)
04040       DR100=100.0*DR9
04050       TYPE 677,DR100
04060   677 FØRMAT(1H ,F4.1,10X,13HMEAN RADIUS   $)
04070       JKL=2
04080       GØ TØ 5
04090   678 R5=R5/(1.0+DR9)
04100       JKL=0
04110   679 IF(DR10.EQ.0.0) GØ TØ 682
04120       RHØ1=RHØ1*(1.0+DR10)
04130       DR100=100.0*DR10
```

```
04140       TYPE 680,DR100
04150   680 FØRMAT(1H ,F4.1,10X,13HBASE RESISTVY$)
04160       JKL=3
04170       GØ TØ 5
04180   681 RH01=RH01/(1.0+DR10)
04190       JKL=0
04200   682 IF(DR11.EQ.0.0) GØ TØ 295
04210       RH02=RH02*(1.0+DR11)
04220       DR100=100.0*DR11
04230       TYPE 683,DR100
04240   683 FØRMAT(1H ,F4.1,10X,13HCLADDING RES $)
04250       JKL=4
04260       GØ TØ 5
04270   684 RH02=RH02/(1.0+DR11)
04280       JKL=0
04290       GØ TØ 295
04300C THE FØURTH PØSSIBILITY ENDS CALCULATIØNS
04310   690 CALL EXIT
04320       END
04330       SUBRØUTINE BESSEL(VAL)
04340       CØMMØN X,Z,Q1,PI
04350       IF(Z.GT.5.0) GØ TØ 1010
04360       K=2.0*Z
04370       L=K+3
04380       F1=0.5*Q1*Q1*Q1
04390       VAL=F1/3.0
04400       DØ 1000 I=1,L
04410       AI=I
04420       F1=-F1*0.25*Z*Z/(AI*AI+AI)
04430       VAL=VAL+F1/(2.0*AI+3.0)
04440  1000 CØNTINUE
04450       GØ TØ 1020
04460  1010 XØ=(((-188.1357/Z+109.1142)/Z-23.79333)/Z+2.050931)/Z
04470       XØ=((XØ-0.1730503)/Z+0.7034845)/Z-0.064109E-3
04480       X1=(((-5.817517/Z+2.105874)/Z-.6896196)/Z+.4952024)/Z
04490       X1=(X1-0.187344E-2)/Z+0.7979095
04500       VAL=(1.0-SQRT(Z)*(X1*CØS(Z-PI/4.0)-XØ*SIN(Z-PI/4.0)))/
04510      1(X*X*X)
04520  1020 RETURN
04530       END
04540       SUBRØUTINE PHASET(A,B,C,V1,Ø3)
04550       DIMENSIØN A(3,5),B(3,5),C(3,5)
04560       Ø1=A(2,5)*SIN(B(2,5))-A(2,1)*SIN(B(2,1))
04570       Ø2=-(A(2,5)*CØS(B(2,5))-A(2,1)*CØS(B(2,1)))
04580       Ø3=ATAN2(Ø1,Ø2)
04590       V1=A(2,1)*SIN(Ø3+B(2,1))
04600       DØ 2000 I=1,3
04610       DØ 2000 J=1,5
04620  2000 C(I,J)=Ø3-ATAN2(V1,SQRT(A(I,J)*A(I,J)-V1*V1))+B(I,J)
04630       RETURN
04640       END
04650       SUBRØUTINE SENS(Ø,RAD,Ø1)
04660       DIMENSIØN Ø(3,5)
04670       Ø9=Ø(1,1)
04680       ØØ=Ø(1,1)
04690       DØ 3010 I=2,5
04700       IF(Ø(1,I).LT.Ø9) GØ TØ 3000
04710       Ø9=Ø(1,I)
04720  3000 IF(Ø(1,I).GT.ØØ) GØ TØ 3010
```

```
04730       00=0(1,I)
04740 3010 CONTINUE
04750       01=(0(1,1)+0(1,2)+0(1,3)+0(1,4)+0(1,5))/5.0
04760       01=01-(0(3,1)+0(3,2)+0(3,3)+0(3,4)+0(3,5))/5.0
04770       XL0=09-00
04780       PERCT=100*XL0/01
04790       DEGR1=01*RAD
04800       DEGR2=XL0*RAD
04810       TYPE 3020,01,XL0,PERCT
04820 3020 FORMAT(1H ,12HPHASE SHIFT=,1PE12.5,2X,8HLIFT0FF=,
04830      11PE12.5,2X,2H%=,1PE12.5)
04840       TYPE 3030,DEGR1,DEGR2
04850 3030 FORMAT(1H ,7HDEGREE:,1PE13.5,5X,1PE13.5)
04860       RETURN
04870       END
04880       SUBROUTINE GAGER(RES)
04890       COMMON /B3/G,D1,D2,RLN,T5,N1,J1,D,E
04900       PI=3.1415926536
04910       IF(J1.EQ.1) GO TO 4015
04920       N1=-1
04930       D3=0.95*SQRT((D2-D1)*RLN/T5)
04940       X2=1.0371E-5/(D3*D3)
04950       Q=40.0
04960 4000 G=40.0+10.0*(ALOG(X2)-ALOG(.9989+.017*(Q/10.0-1.0)))/2.3
04970      10259
04980       IF(ABS(Q-G).LT.1.0E-4) GO TO 4010
04990       Q=G
05000       GO TO 4000
05010 4010 IG=G
05020       G=IG
05030 4015 X2=(.9989+.017*(G/10.0-1.0))*10.0**(G/10.0-4.0)
05040       D3=SQRT(1.0371E-5/X2)
05050       IF(G.GT.40.0) GO TO 4020
05060       X3=(.460655*ALOG(D3*1.E3)-.43444)*1.E-3
05070       GO TO 4030
05080 4020 X3=(98.02228*D3+2.56791E-2)*1.E-3
05090 4030 ID=(RLN/(D3+X3))
05100       D=ID
05110       IE=(D2-D1)/(D3+X3)
05120       E=IE
05130       IF(N1.EQ.-1) GO TO 4040
05140       T5=D*E
05150 4040 RES=T5*X2*(D2+D1)*PI/12.0
05160       RETURN
05170       END
05180       SUBROUTINE CIRCT(TMAG,PHASE,Q0,T1,T2)
05190       COMMON /B1/R1,R2,R3,R4,RL3,RL4,R0,R6,R7,R9,C6,C7,V0,GAIN
05200       COMMON /B1/W,FREQ,RBAR,TURNS1,TURNS2/B2/TMUT,DRIVER
05210       COMMON /B2/PICKUP,AIR1,AIR2
05220       COMPLEX TMUT,DRIVER,PICKUP,Z1,Z2,Z3,Z4,Z5,Z6,Z7
05230       COMPLEX DENOM,TNUM,VOLT
05240       DIMENSION TMUT(3,5),DRIVER(3,5),PICKUP(3,5)
05250       DIMENSION TMAG(3,5),PHASE(3,5)
05260       T1=TURNS1/((R2-R1)*RL3)
05270       T2=TURNS2/((R4-R3)*RL4)
05280       Q0=6.300475204E-7*FREQ*RBAR
05290       Z1=CMPLX(W*R0*C6,-1.0)
05300       Z2=CMPLX(W*R9*C7,-1.0)
05310       Z3=CMPLX(0.0,-R0)
```

```
05320       Z4=CMPLX(0.0,-R9)
05330       D0 5000 I=1,3
05340       D0 5000 J=1,5
05350       Z5=Q0*T1*T2*TMUT(I,J)
05360       Z6=Q0*T1*T1*(0.0,1.0)*(DRIVER(I,J)+AIR1)
05370       Z7=Q0*T2*T2*(0.0,1.0)*(PICKUP(I,J)+AIR2)
05380       DEN0M=Z1*Z2*Z5*Z5+(Z1*(Z6+R6)+Z3)*
05390      5 (Z2*(Z7+R7)+Z4)
05400       TNUM=V0*R9*GAIN*(0.0,-1.0)*Z5
05410       V0LT=TNUM/DEN0M
05420       TMAG(I,J)=CABS(V0LT)
05430 5000  PHASE(I,J)=ATAN2(AIMAG(V0LT),REAL(V0LT))
05440       RETURN
05450       END
05460       SUBR0UTINE CIRCT1(01,V1,0,RAD,SEN)
05470       DIMENSI0N 0(3,5),TMAG(3,5),PHASE(3,5)
05480       CALL CIRCT(TMAG,PHASE,Q0,T1,T2)
05490       Q1=0.0
05500       D0 6000 I=1,3
05510       D0 6000 J=1,5
05520       Q2=01-ATAN2(V1,SQRT(TMAG(I,J)*TMAG(I,J)-V1*V1))
05530      1+PHASE(I,J)-0(I,J)
05540       IF(ABS(Q1).GT.ABS(Q2)) G0 T0 6000
05550       Q1=Q2
05560 6000  C0NTINUE
05570       Q2NEW=RAD*Q1
05580       Q3=100.0*Q1/SEN
05590       TYPE 6010,01,Q2NEW,Q3
05600 6010  F0RMAT(1H+,1X,2(1PE12.5,2X),1PE12.5)
05610       RETURN
05620       END
```

VITA

Jackie T. Hill was born in Virginia Beach, Virginia, on March 7, 1948. He attended elementary school and graduated from Princess Anne County High School in 1965. In September 1965 he entered Virginia State College in Petersburg, Virginia, and received a Bachelor of Science degree in Physics in May 1969. He was employed by the Union Carbide Corporation-Nuclear Division in Oak Ridge, Tennessee on June 9, 1969 as an Associate Physicist. He is presently with the Nondestructive Testing Department at the Union Carbide Corporation Y-12 Plant. He is a member of the American Society of Nondestructive Testing (ASNT). He is also a member of Sigma Pi Sigma.

He entered the Graduate School at The University of Tennessee in 1970, and received his Master of Science degree with a major in Physics in 1974.

He is married to the former Jacqueline Ernestine Batts of Petersburg, Virginia.